



# Master's Thesis Defense

## Finite Element Analysis for the Damage Detection of Light Pole Structures

Qixiang Tang

Master's Candidate

Advisor: Prof. TzuYang Yu

Department of Civil and Environmental Engineering

The University of Massachusetts Lowell

Lowell, Massachusetts, 01854

July 18<sup>th</sup>, 2014

# Outline

- Introduction
- Objective
- Literature Review
- Approach
- Finite Element Modeling
- Results and Discussion
- Proposed Damage Detection Methodology
- Conclusions
- Contributions
- Future Work
- References
- Acknowledgement

# Introduction

In December 2009, a 200-pound corroded light pole fell across the southeast expressway in Massachusetts.[1]



(Source: [1] I-team: Aging light poles a safety concern on mass. roads)

# Introduction

1. Failure of light poles are **critical** as they are typically located adjacent to roadways, highway and bridges.
2. Failures of aging light poles can jeopardize the **safety of residents** and damage adjacent **structures**. (e.g., residential houses, and electricity boxes.)



(Photo source: [www.news-leader.com](http://www.news-leader.com))



(Photo source: [www.news-leader.com](http://www.news-leader.com))

Therefore, aging light poles need to be repaired or removed before residents get hurt.

# Objective

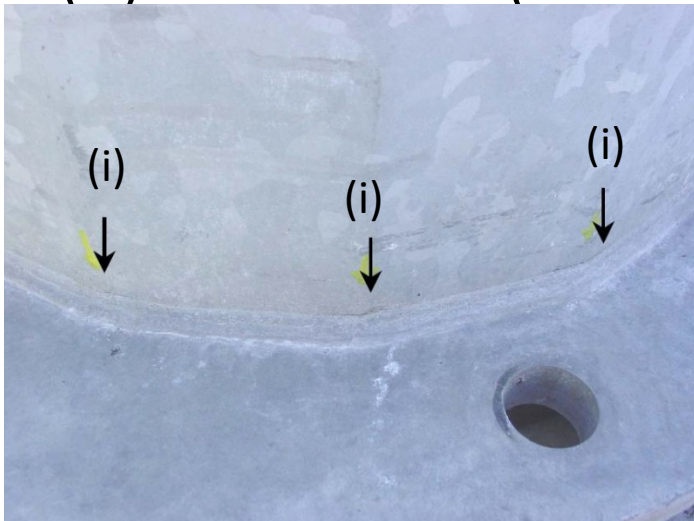
To develop a damage detection methodology for light pole structures using modal frequencies and mode shapes extracted from their free vibration responses

# Literature Review

- How do damages affect light poles in terms of mechanical responses?
- Where do damages usually occur in a light pole?
- How can we locate and quantify damages using the mechanical responses of light pole?

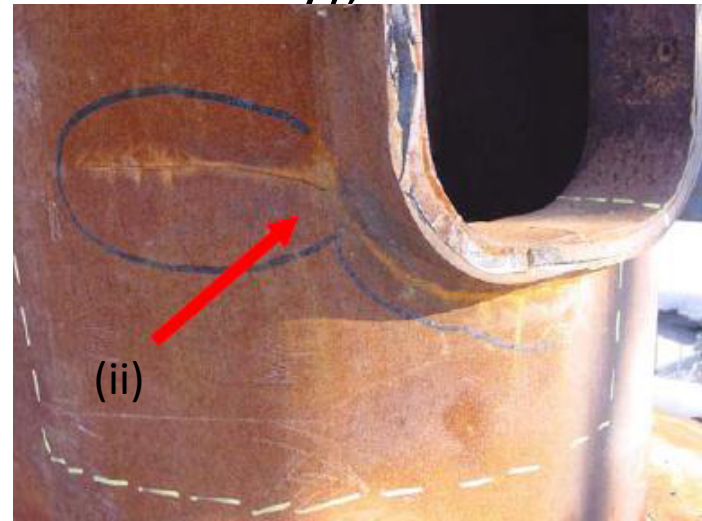
# Literature Review

1. There are three most common/possible damage locations in light poles (Garlich and Thorkildsen (2005) [14] , Caracoglia and Jones (2004)[7]; Conner et. al. (2005)[6])
  - (i) pole-to-baseplate connection,
  - (ii) handhole detail, and
  - (iii) anchor bolts (not considered in this study);



Cracks at bottom of the pole

(Photo source: <http://polesafety.com>)



Cracks at handhole detail

(Photo source: <http://polesafety.com>)

# Literature Review

2. Changes in modal frequencies and mode shapes are expected while introducing damages into structures. (Lee and Chung (2000) [44]; Abdo and Hori (2002)[4])

For example, the modal frequency of an undamped single degree of freedom (SDoF) structure can be determined by following equation:  $\omega = \sqrt{k/m}$

where  $\omega$  is the modal frequency,  $k$  is stiffness of the structure, and  $m$  is mass of structure.

Since the presence of damages reduces  $k$  ( stiffness) of the structure.

Consequently,  $k \downarrow \longrightarrow \omega \downarrow$



# Literature Review

3. Structural damages in light poles can be simulated by reducing materials' properties (i.e. Young's modulus) in numerical simulation. (Yan *et. al.* (2006) [42])

For example, the stiffness of a cantilever beam (SDoF) can be written as:

$$k=3EI/h^3$$

where  $E$  is Young's modulus of material, and  $I$  is the mass moment of inertia, and  $h$  is the height of this beam.



# Literature Review

4. Experimentally capturing dynamic characteristics (such as modal frequencies and mode shapes) of light poles is difficult and time consuming. (Yan *et. al.* (2007)[43])

# Literature Review

- How do damages affect light poles in terms of mechanical responses?
  - There will be changes in modal frequencies and mode shapes.
- Where do damages usually appear in a light pole?
  - There are three common damage locations.
- How can we locate and quantify damages using the mechanical response of light poles?
  - Need a damage detection method.
  - Use numerical simulation to develop the method.

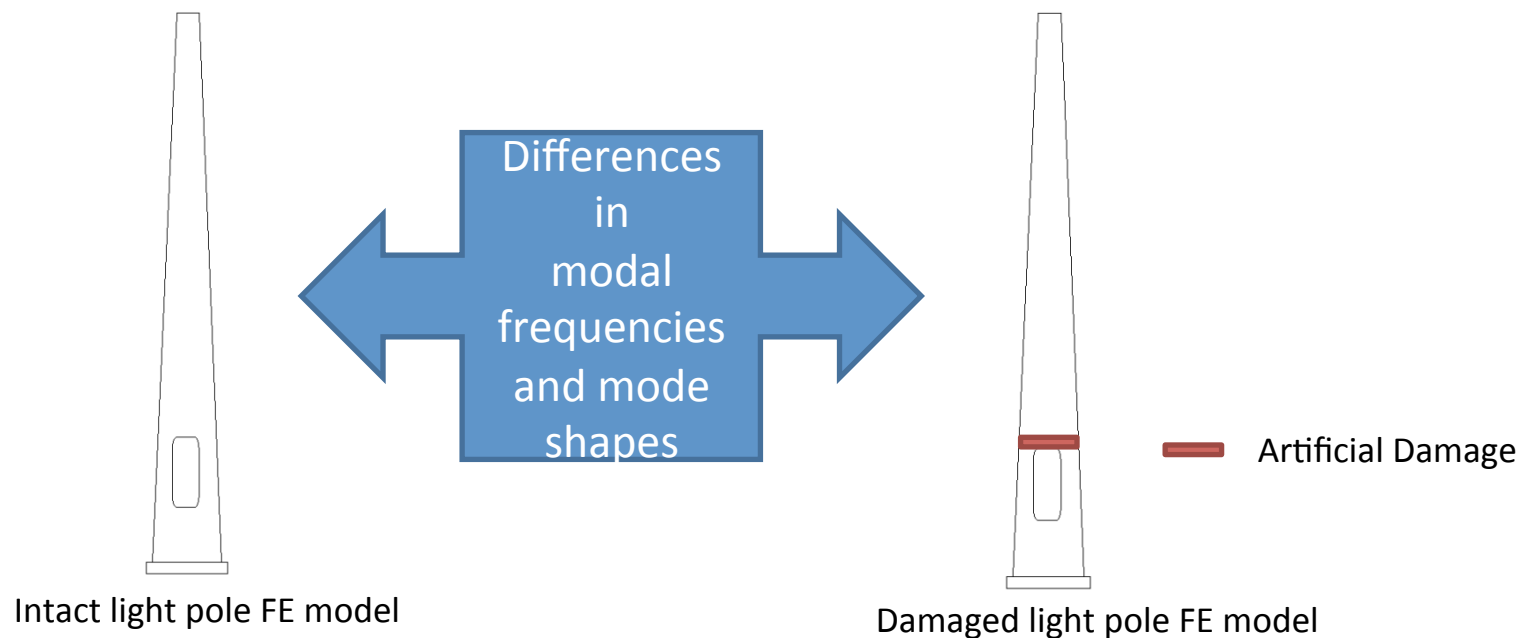
# Approach

**Proposed research approach is determined based on:**

1. Assuming damages only occur at three most common damage locations.
2. Using dynamic responses (i.e., modal frequencies and mode shapes) as parameters for investigating differences between intact and damaged light poles.
3. Using numerical methods (i.e., finite element (FE) method).

# Approach

Simulate intact and damaged light poles by the FE method, and study the differences in modal frequencies and mode shapes between intact and artificially damaged FE models.

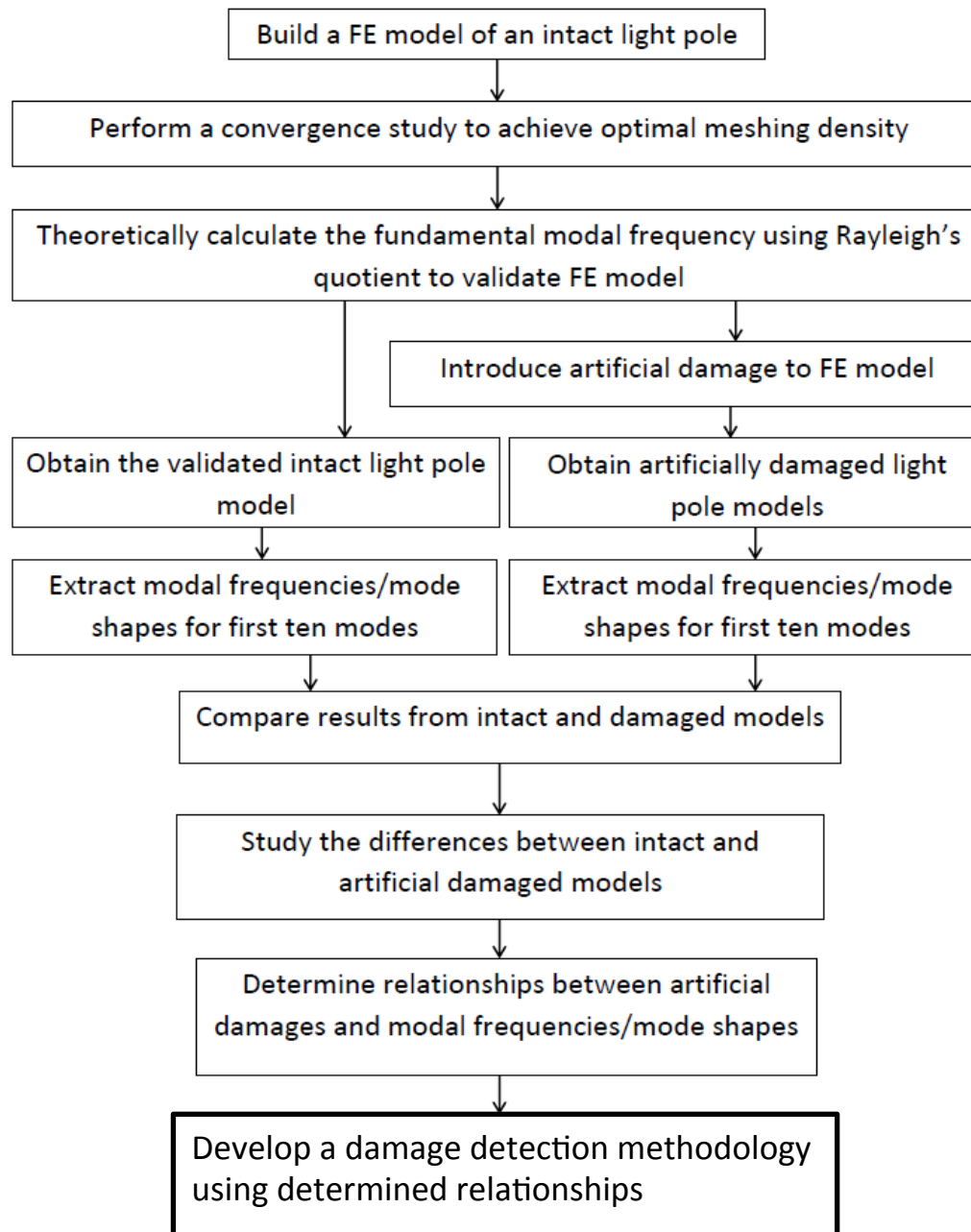


# Approach

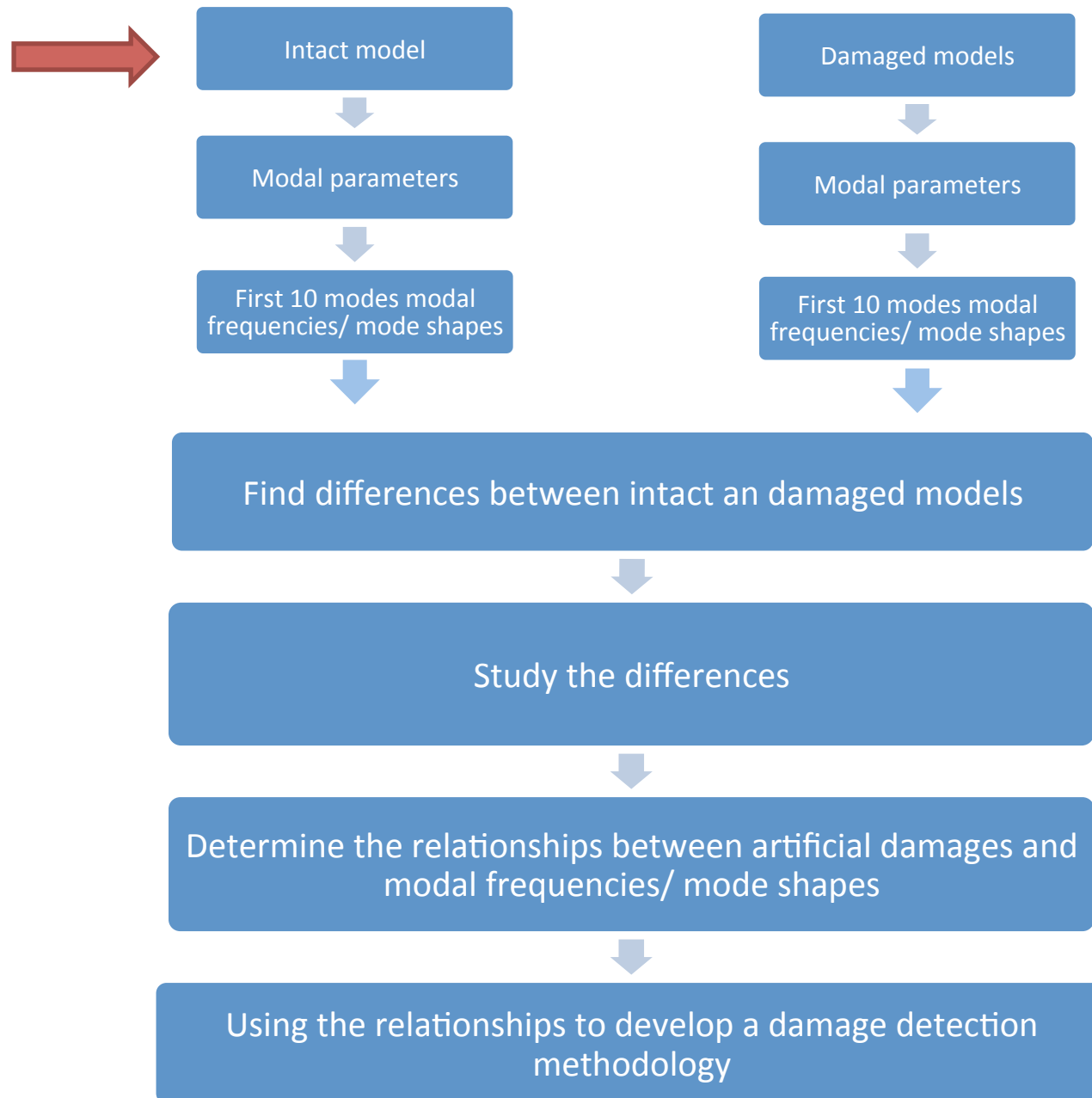
Assumptions :

- First ten modal frequencies are available.
- FE light poles are undamped.
- Damages only occur at pole-to-baseplate connection, and handhole detail.
- There is only one damage in each artificially damaged light pole model.
- A commercial FE package ABAQUS<sup>®</sup> (Dassault Systèmes) is used.

# Research Methodology



# Roadmap



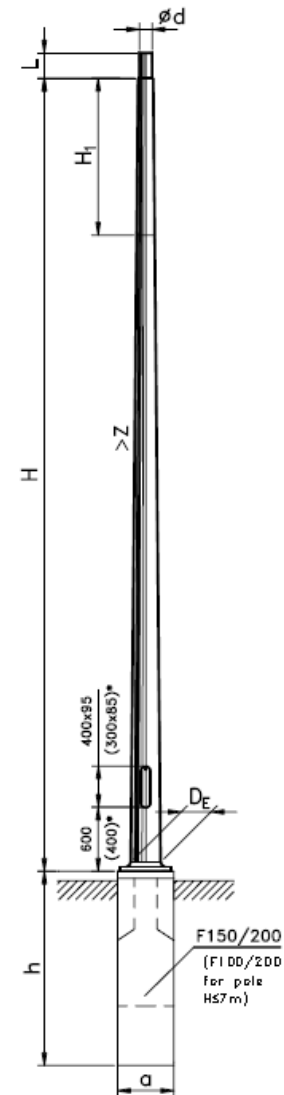


# Finite Element Modeling

## Configurations of an Example Light Pole



(source: ELEKTROMONTAŻ RZESZÓW SA: *Lighting poles and masts*, 2009 )



\*- dimensions for pole H $\leq$ 7m

# Finite Element Modeling

Technical data

TYPE	H	t <sub>bl</sub>	H <sub>1</sub>	∅d/D <sub>E</sub>	L	m	S	axaxh Type
	m	mm	m	mm	mm	kg	m <sup>2</sup>	m
S-60SRwP/4	6		2,0	48; 60/140		68,0	1,47	0,3x0,3x1,0
S-70SRwP/4	7		2,0			79,0	1,71	F100/200
S-80SRwP/4	8		2,2			96,0	2,76	
S-90SRwP/4	9	4	2,5		100	104,0	3,41	
S-100SRwP/4	10		3,5	48; 60/170		110,0	3,65	0,3x0,3x1,5
S-110SRwP/4	11		2,2			128,0	3,89	F150/200
S-120SRwP/4	12		3,2			135,0	4,22	

Note: H<sub>1</sub> – reduction piece for straight pole is ordered as separate element.

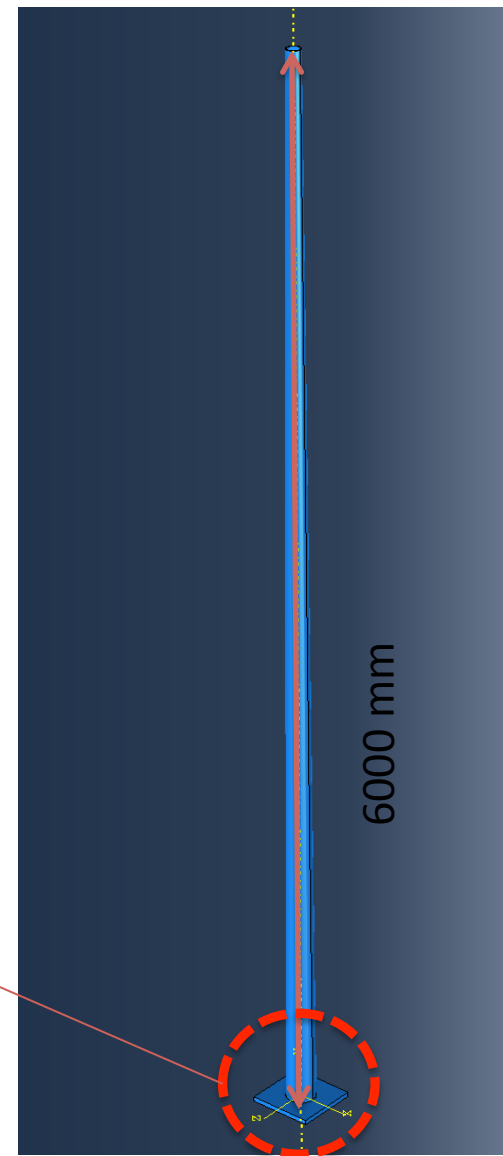
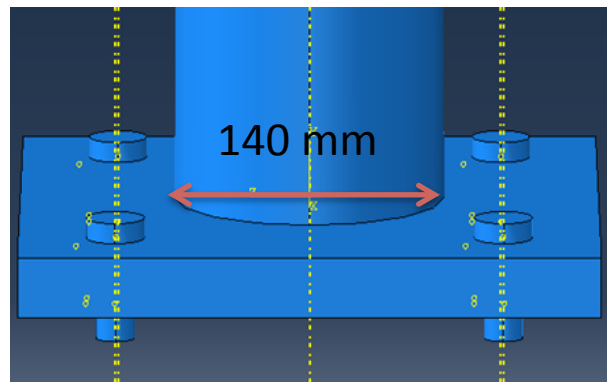
(source: ELEKTROMONTAŻ RZESZÓW SA: *Lighting poles and masts*, 2009 )

-- Chosen geometry

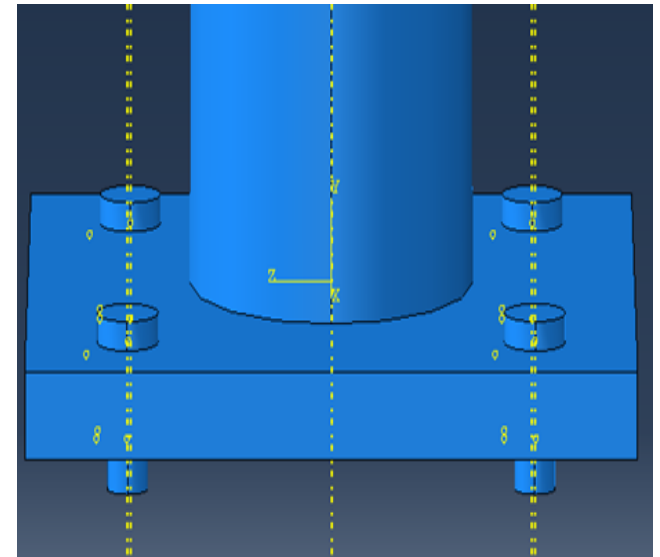
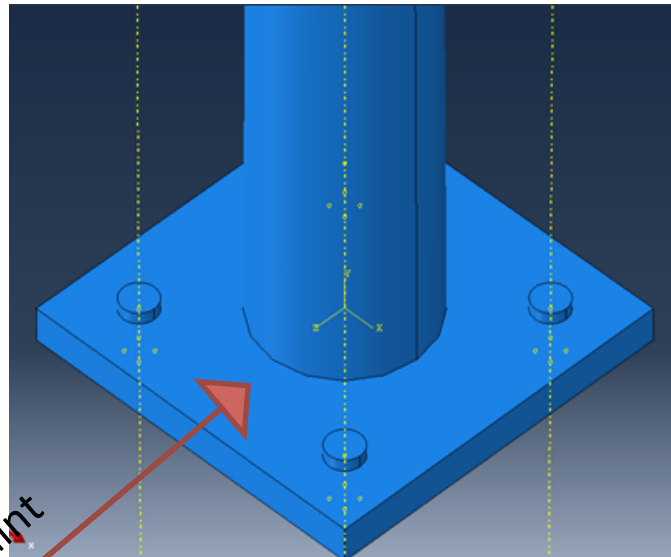
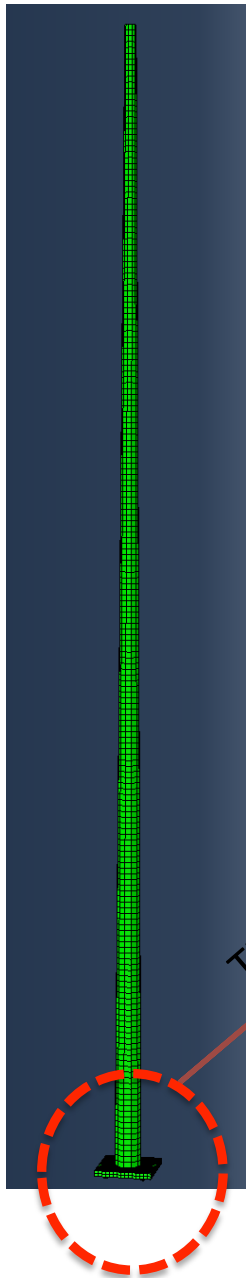
# Finite Element Modeling

## Materials (steel) & Geometries

Density:	7.85E-09 ton/mm <sup>3</sup>
Young's Modulus:	207,000 MPa
Poisson's ratio:	0.3
Yield stress:	450 MPa
Length of the pole:	6,000 mm
Diameter at top:	60 mm
Bottom:	140 mm



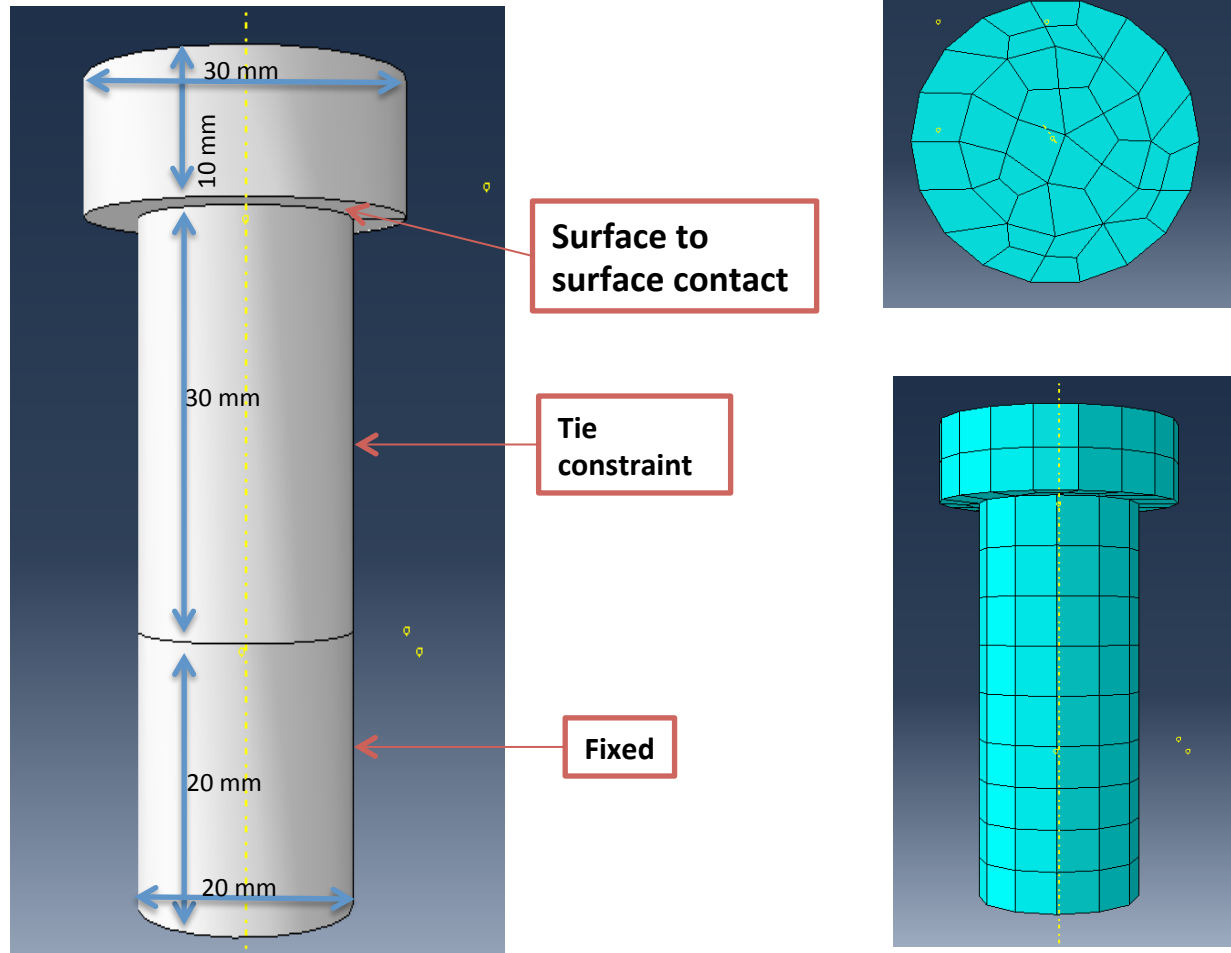
# Baseplate Model



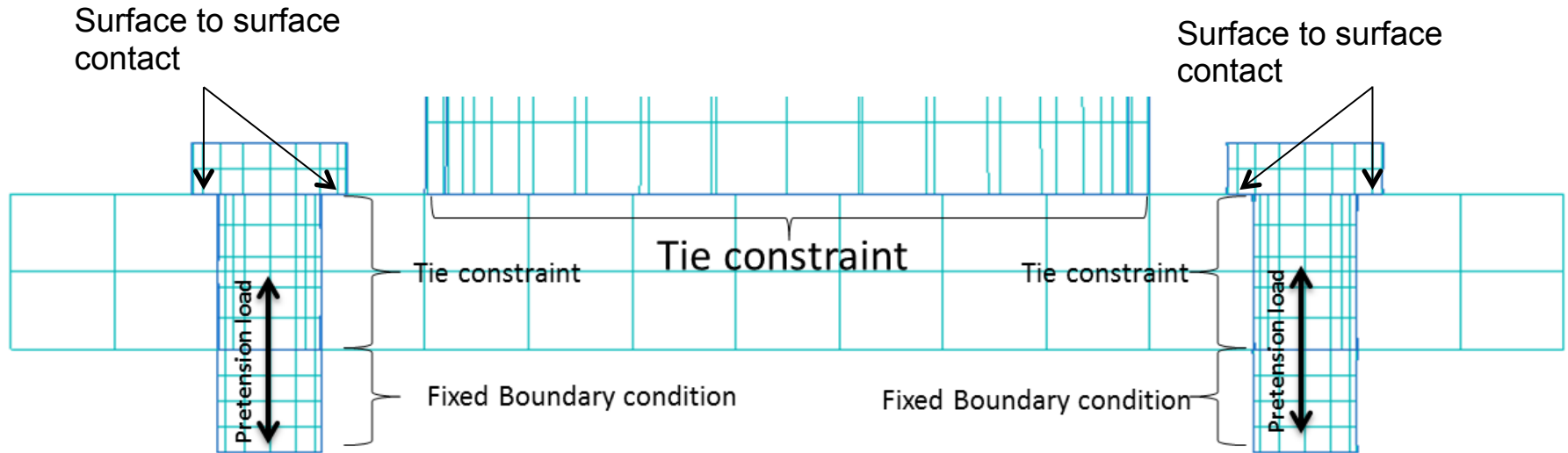
Tie constraint

- Baseplate size: L x W x H: 300x300x30 (mm)
- Boundary condition: Tie constraint is used to assemble the pole and the baseplate.

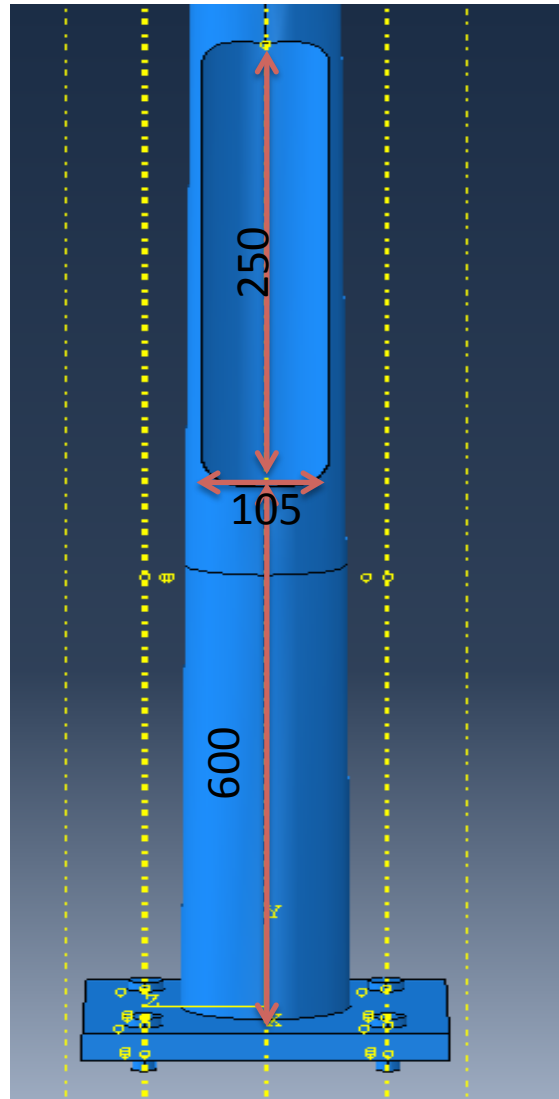
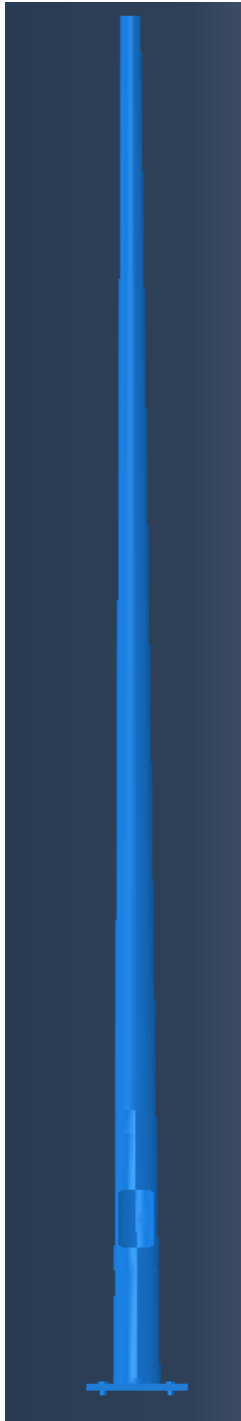
# Bolt Models



# Baseplate Model



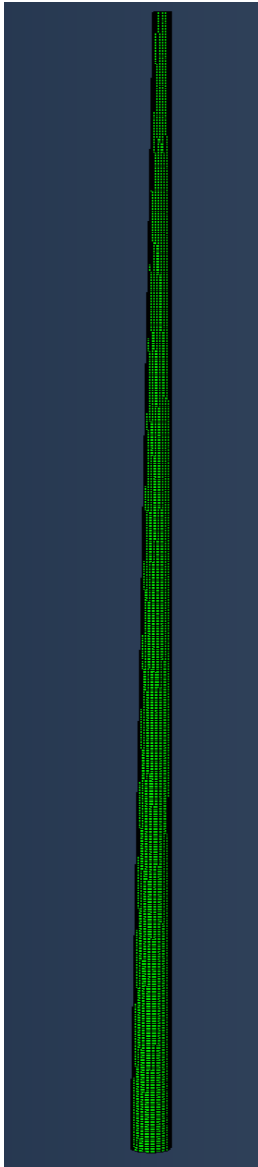
# Handhole



Handhole size:  
250x105

(Dimension: mm)

# Verification of an Intact FE Pole Model



An intact FE pole model was verified by comparing the first modal frequency between the FE result and theoretical calculation.

First modal frequency of the FE pole model created in ABAQUS® is : **4.236 Hz (FE result)**.

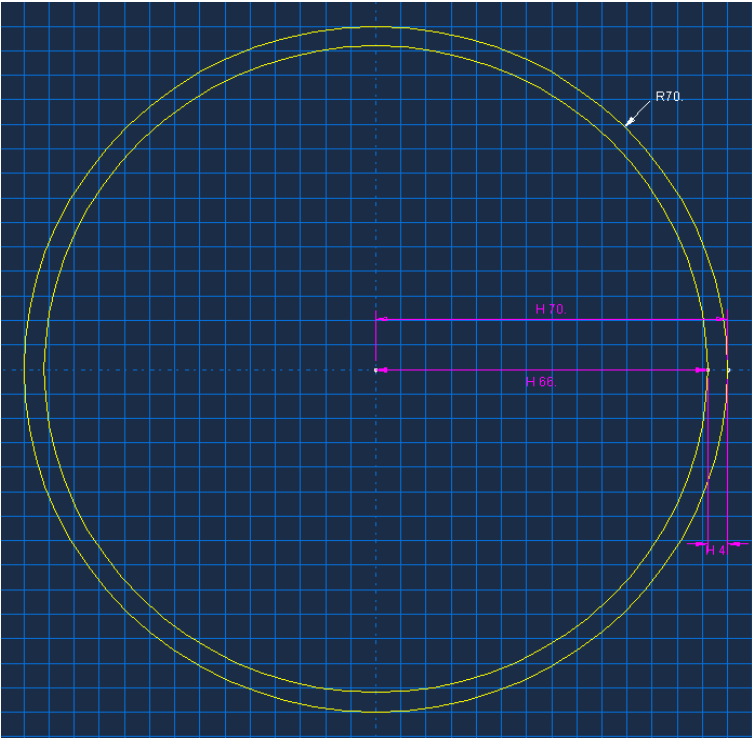
0	Increment	0: Base State		
1	Mode	1: Value = 708.22	Freq = 4.2355	(cycles/time)
2	Mode	2: Value = 708.22	Freq = 4.2355	(cycles/time)
3	Mode	3: Value = 14192.	Freq = 18.960	(cycles/time)
4	Mode	4: Value = 14192.	Freq = 18.960	(cycles/time)
5	Mode	5: Value = 89791.	Freq = 47.691	(cycles/time)
6	Mode	6: Value = 89791.	Freq = 47.691	(cycles/time)



# Theoretical Calculation

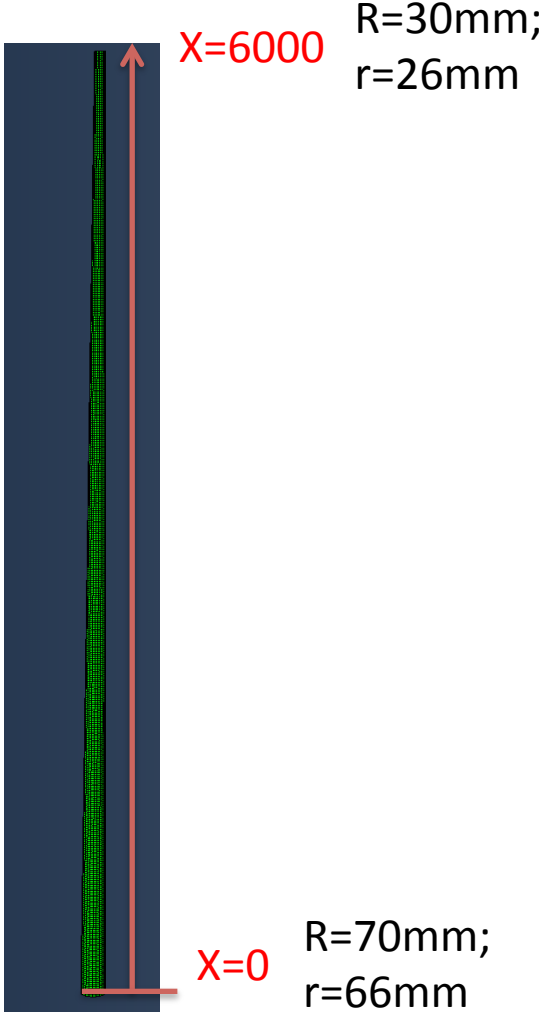
Given:

- Density: 7.85E-09 Ton/mm<sup>2</sup>
- Young's Modulus: 207000 MPa
- Poisson's ratio: 0.3
- Yield strength: 450 MPa
- Length of the pole: 6000 mm



Cross section at bottom of the pole(x=0)

R=70mm;  
r=66mm



# Theoretically Computed First Modal Frequency

## 1. Radius functions

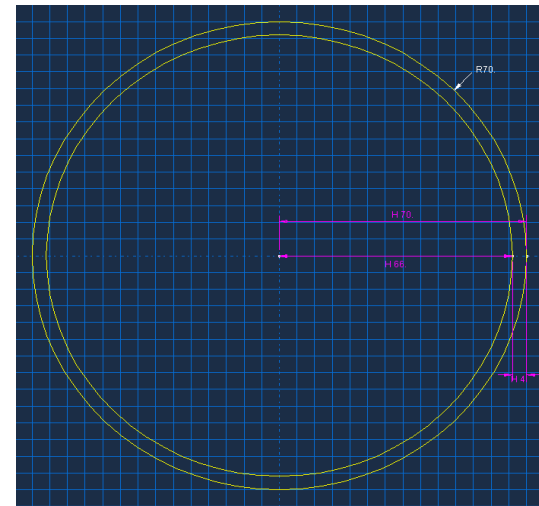
Radius of external edge:  $R(x) = \frac{1}{-150} \cdot x + 70$

Radius of internal edge:  $r(x) = R(x) - 4$

## 2. Distribution functions for mass and mass moment of inertia

$$m(x) = \pi \cdot (R(x)^2 - r(x)^2) \cdot 7.85 \cdot 10^{-9}$$

$$I(x) = \left( R(x)^4 - r(x)^4 \right) \cdot \frac{\pi}{4}$$



# Theoretically Computed First Modal Frequency

## 3. Generalized mass, and generalized stiffness

$$m' = \int_0^L m(x) \psi(x)^2 dx$$
$$k' = \int_0^L E \cdot I(x) \cdot \left( \frac{d^2 \psi(x)}{dx^2} \right)^2 dx$$

Eq. 8.3.12

Anil K Chopra. *Dynamics of structures-Theory and applications to earthquake engineering*. Pg.312

where  $\psi(x)$  is shape function of cantilever beams. **The best-fit shape function** is the one which provides **lowest value** of first modal frequency among three given shape functions.

# Theoretically Computed First Modal Frequency

First modal frequency:  $\omega := \left( \frac{k'}{m'} \right)^{0.5}$

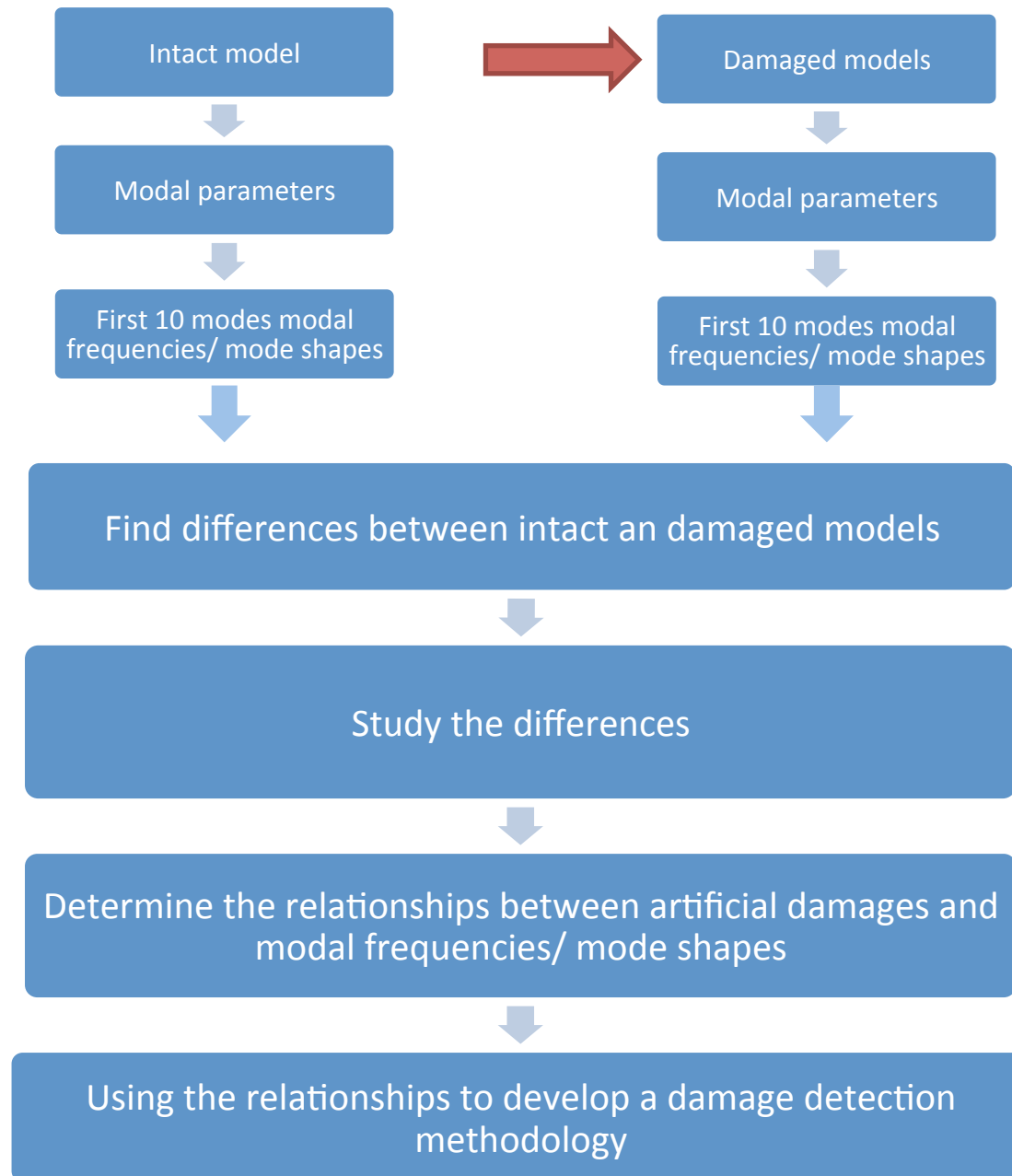
Shape function	$\psi(x) := \frac{3x^2}{2 \cdot 6000^2} - \frac{x^3}{2 \cdot 6000^3}$	$\psi(x) := 1 - \cos\left(\frac{\pi \cdot x}{2 \cdot 6000}\right)$	$\psi(x) := \frac{x^2}{6000^2}$
f (Hz)	4.361	4.298	4.396

**Theoretical result:** The lowest value of first modal frequency is **4.298 Hz**.

**FE result: 4.236 Hz**

→ Only 1.4% of difference. This means the FE result is correct and accurate.

# Roadmap



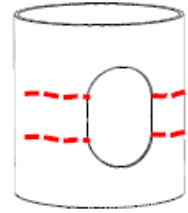
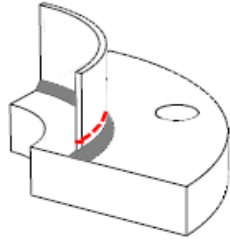
# Finite Element Models

## Damaged models

Damaged models were simulated by introducing artificial damages to intact light pole models.

# Damage Simulations

Most common damage locations:

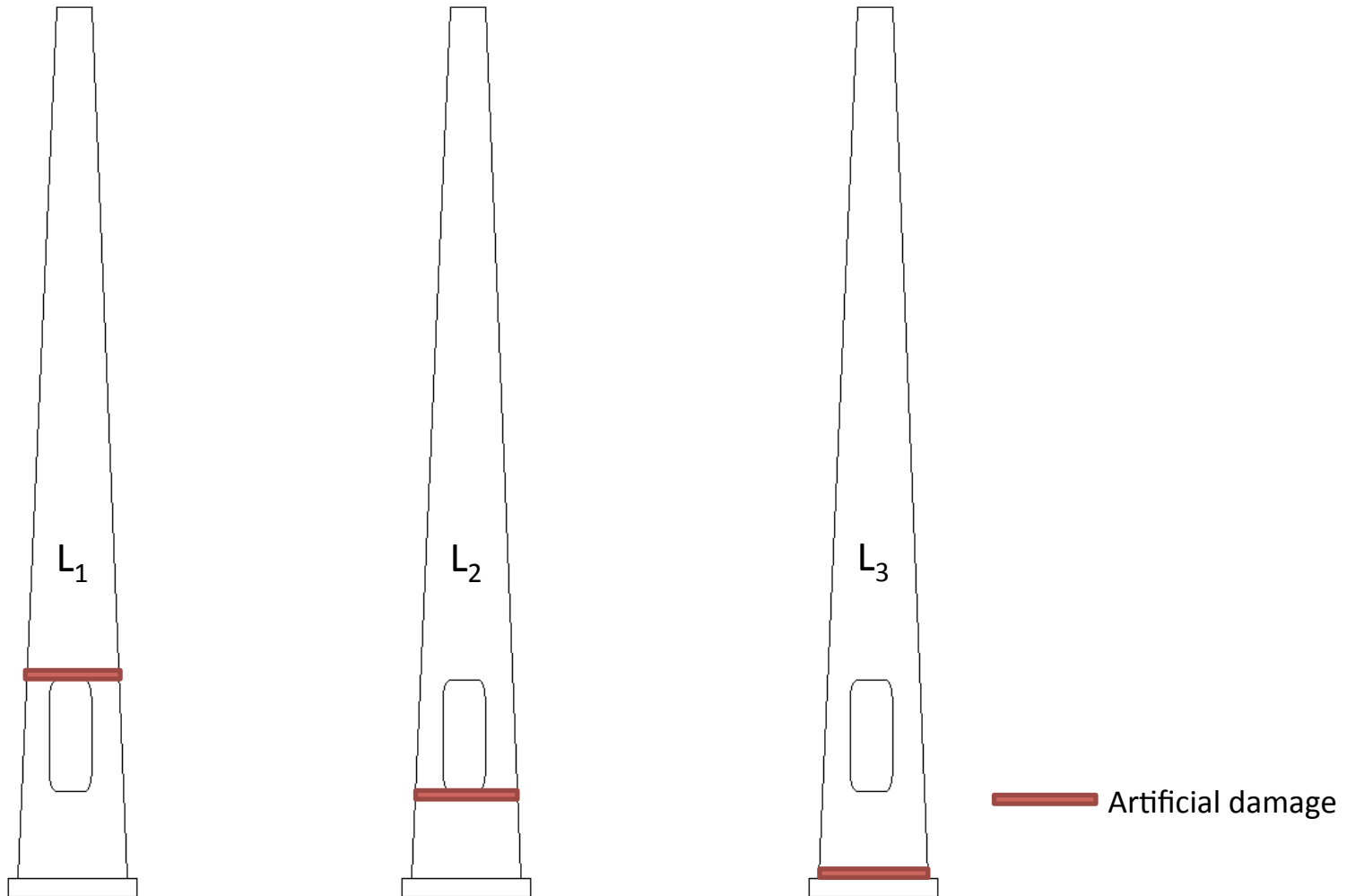
Description	Finite Life Constant, $A \times 10^8$ (ksi <sup>3</sup> (MPa <sup>3</sup> ))	Threshold, ( $\Delta F$ ) <sub>TH</sub> (ksi (MPa))	Potential Crack Location	Illustrative Example
<b>SECTION 3 — HOLES AND CUTOUTS</b>				
3.1 Net section of un-reinforced holes and cutouts.	250.0 (85200)	24.0 (165)	In tube wall at edge of unreinforced handhole.	
4.6 Full penetration groove-welded tube-to-transverse plate connections welded from both sides with back-gouging (without backing ring).	$K_F \leq 1.6 : 11.0$ (3750) $1.6 < K_F \leq 2.3 : 3.9$ (1330)	$K_I \leq 3.2 : 10.0$ (69) $3.2 < K_I \leq 5.1 : 7.0$ (48) $5.1 < K_I \leq 7.2 : 4.5$ (31)	In tube wall at groove-weld toe.	

(Source: NCHRP Report, Cost-Effective Connection Details for Highway Sign, Luminaire, and Traffic Signal Structures)

# Damage Simulations

1. Location ( $L_j$ ):

Artificial damages have three damage location:  $L_1$ ,  $L_2$  and  $L_3$ .

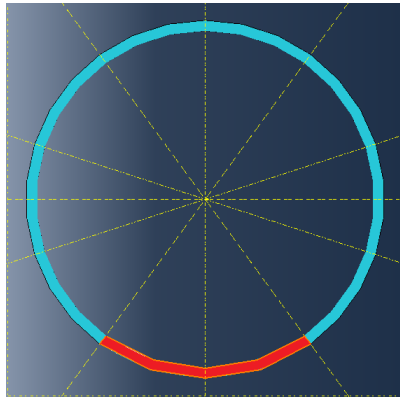




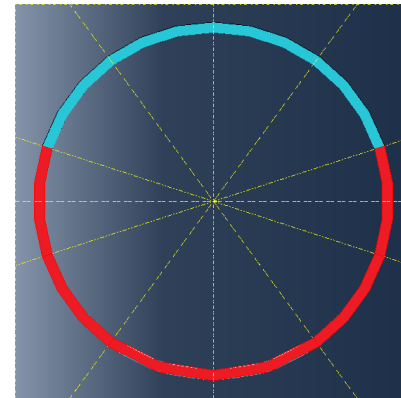
# Damage Simulations

## 2. Damage sizes ( $\Delta A$ ):

Artificial damages have **five** different sizes, including:  $\Delta A \in [0.2A, 0.4A, 0.6A, 0.8A, 1.0A]$ , where  $A$  is the total cross-sectional area.



0.2A – 20% Cross-sectional area is damaged  
(at location L3)



0.6A -- 60% Cross-sectional area is damaged  
(at location L3)

— Artificial damage

# Damage Simulations

## 3. Damage level ( $\Delta E$ ):

Damages are simulated by reducing Young's Modulus in damaged regions. There are five levels:  $\Delta E \in [0.1, 0.3, 0.5, 0.7, 0.9] * E$ , where  $E$  is the Young's modulus of materials.

Group A														
$\Delta E=50\%$ of Youngs modulus														
$\Delta A=20\%$			$\Delta A=40\%$			$\Delta A=60\%$			$\Delta A=80\%$			$\Delta A=100\%$		
Scenario A-1			Scenario A-2			Scenario A-3			Scenario A-4			Scenario A-5		
$L_1$	$L_2$	$L_3$	$L_1$	$L_2$	$L_3$	$L_1$	$L_2$	$L_3$	$L_1$	$L_2$	$L_3$	$L_1$	$L_2$	$L_3$

Group B														
$\Delta A=100\%$ of total area														
$\Delta E=90\%$			$\Delta E=70\%$			$\Delta E=50\%$			$\Delta E=30\%$			$\Delta E=10\%$		
Scenario B-1			Scenario B-2			Scenario B-3			Scenario B-4			Scenario B-5		
$L_1$	$L_2$	$L_3$	$L_1$	$L_2$	$L_3$	$L_1$	$L_2$	$L_3$	$L_1$	$L_2$	$L_3$	$L_1$	$L_2$	$L_3$

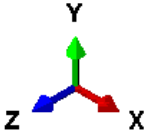
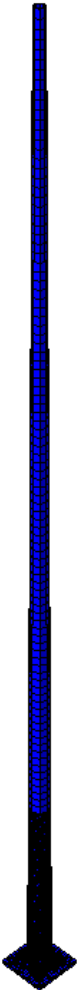
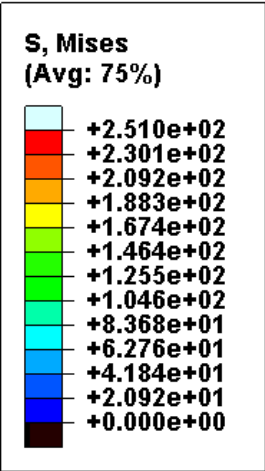
Obtain first ten modal frequencies and mode shapes from different damaged models (listed above) and the intact model.

# Damage Simulations

Mode number



Step: Step-1 Frame: 0  
Total Time: 1.000000

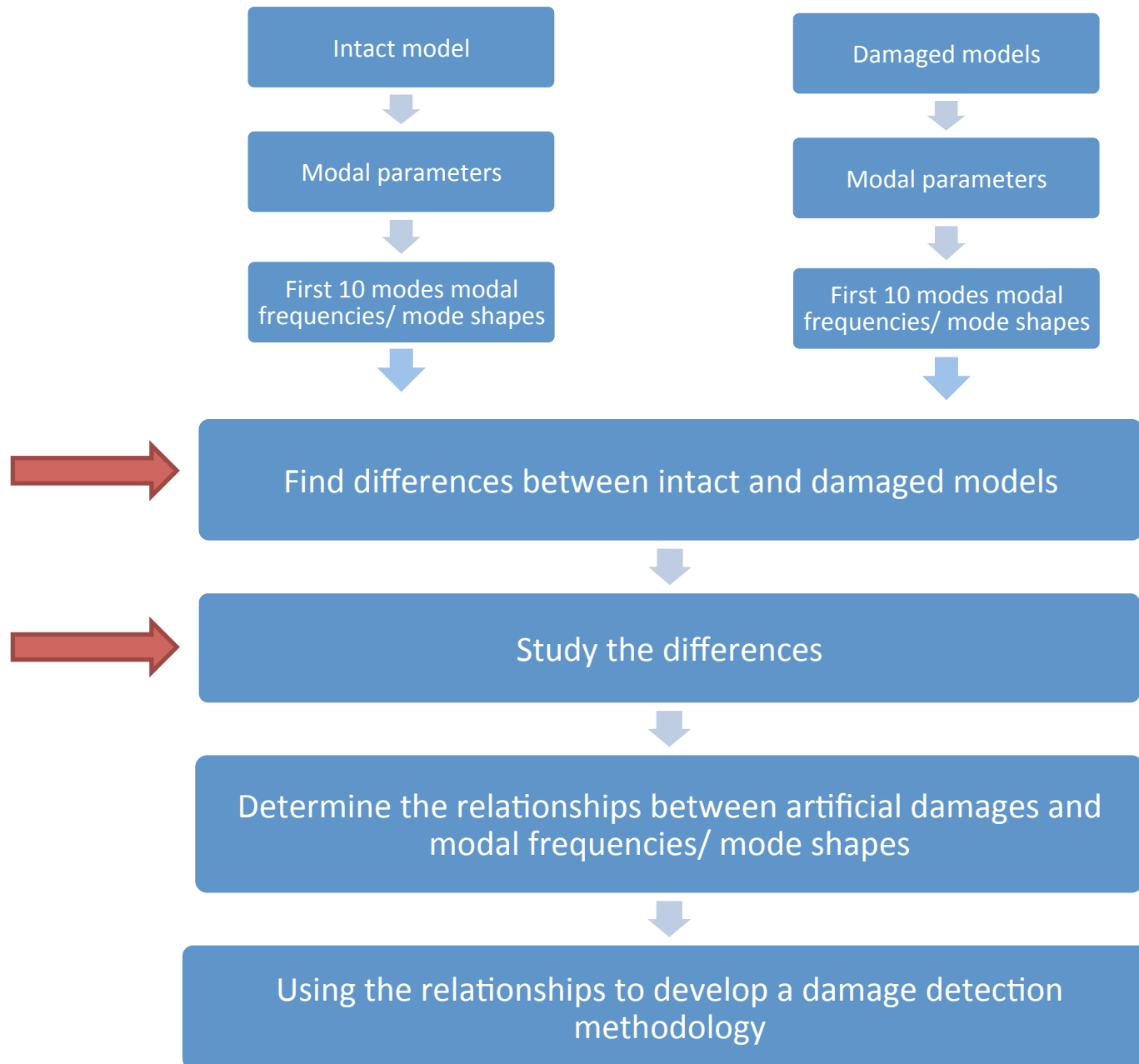


Modal frequency



Step: Step-1  
Increment 0: Base State  
Primary Var: S, Mises  
Deformed Var: U Deformation Scale Factor: +6.050e+02

# Roadmap



# Results and Discussion

## Definition:

When an intact light pole is **known**, **modal frequency difference** can be computed by the following equation:

$$\Delta f_i^j = \frac{(f_i^j|_{intact} - f_i^j|_{damaged})}{f_i^j|_{intact}} * 100\%$$

where  $\Delta f_i^j$  is the modal frequency difference of a damaged pole in  $i^{\text{th}}$  mode with a damage locating at  $L_j$ ,  $f_i^j|_{intact}$  is modal frequency of the intact model, and  $f_i^j|_{damaged}$  is the modal frequency of a damaged model.

# Results and Discussion

## Definition:

Sensitive modes:

Out of the first ten modes, the modes whose modal frequency differences **exceed** a defined threshold value  $t_s$ .

Threshold value  $t_s$  : 1.25 times the average modal frequency differences of the first ten modes.

$$t_s = 1.25 \sum_{i=1}^{10} f_{ij} / 10$$

# Results and Discussion

## Definition:

Insensitive modes:

Out of first ten modes, the modes whose modal frequency differences are **lower** than a defined threshold value  $t_i$ .

Threshold value  $t_i$ : 0.25 times the average modal frequency differences of the first ten modes.

$$t_i = 0.25 \sum_{i=1}^{10} f_{ij} / 10$$



# Results and Discussion

## Definition:

Curvature of mode shapes can be computed by Central Difference equation:

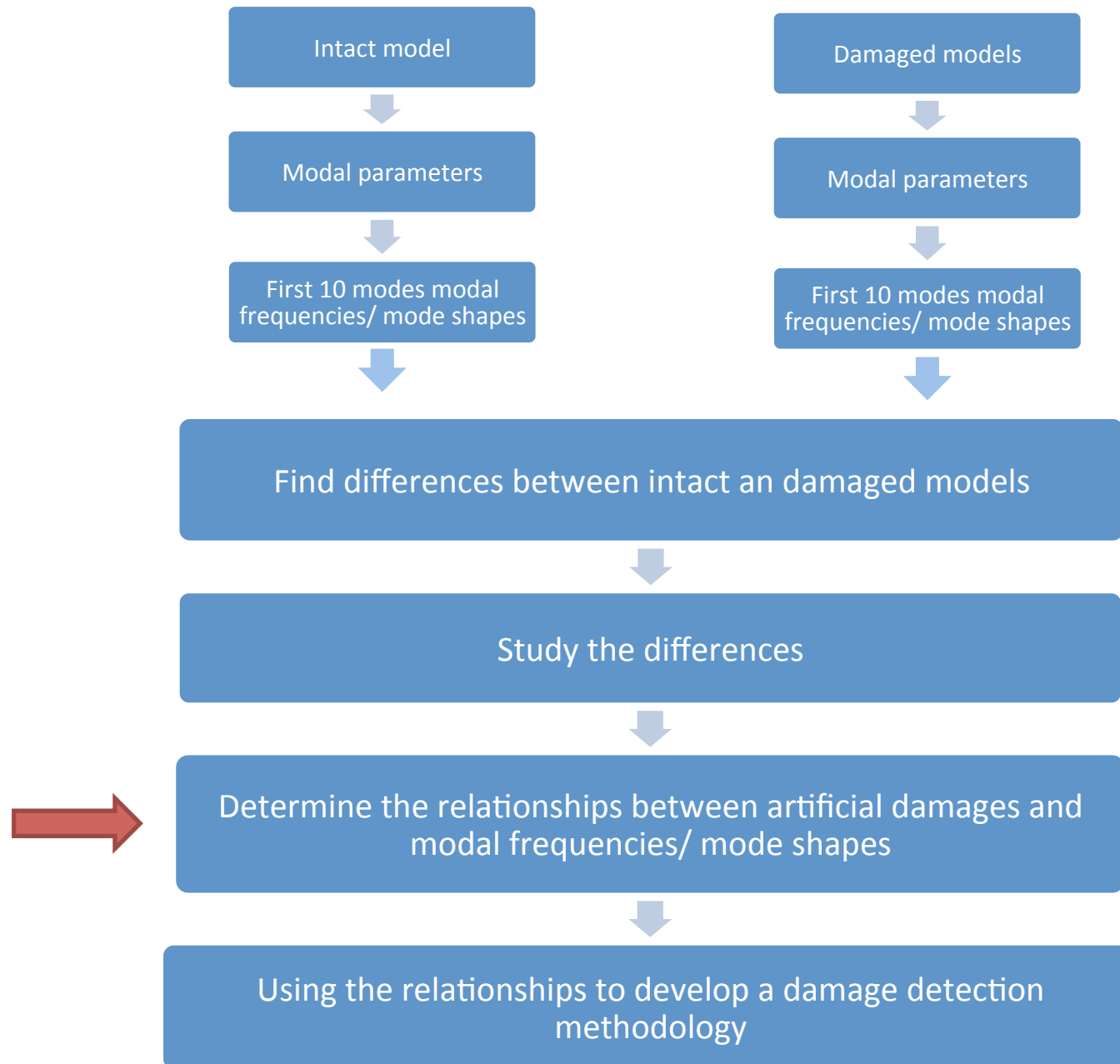
$$\phi''(x)_n = \frac{\phi(x)_{n+1} - 2\phi(x)_n + \phi(x)_{n-1}}{d^2}$$

where  $\phi(x)$  is the displacement of mode shape at node  $n$ ,  $d$  is the distance between two nodes, and  $\phi''(x)$  is the curvature of mode shape at node  $n$ .

Changes in curvature of mode shapes ( $\Delta r_{\phi''}$ ) can be computed by the following equation:

$$\Delta r_{\phi''} = \frac{\phi''_n|_{\text{damaged}}}{\phi''_n|_{\text{intact}}}$$

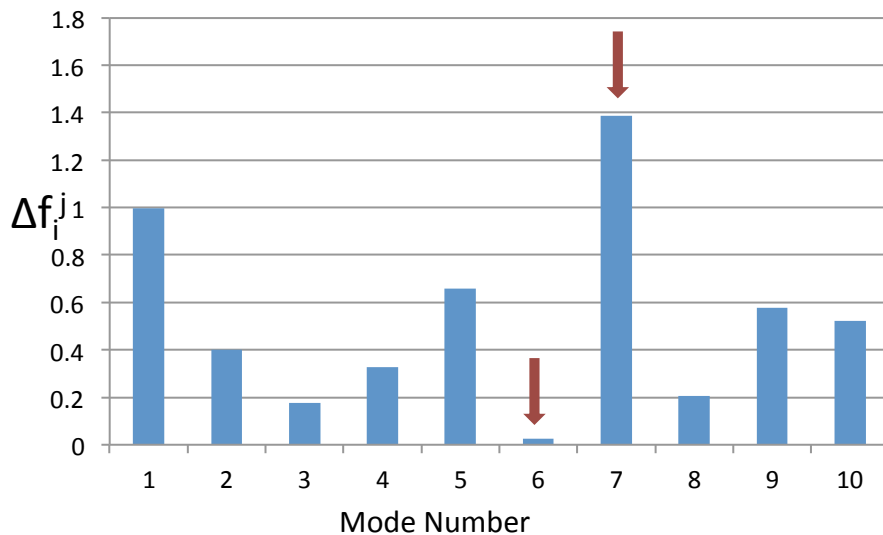
# Roadmap



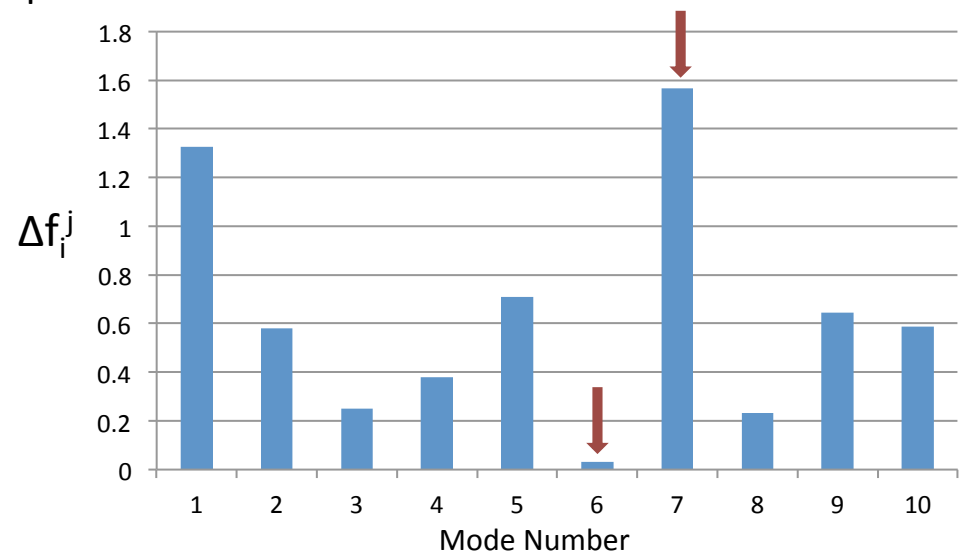
# Summary of FE Results

Three patterns were found from FE results on modal frequencies and mode shapes.

1. In different damage scenarios with same damage location, some modes always have highest/lowest value in modal frequency differences ( $\Delta f_i^j$ ).



Damage location: L1  
Damage size: 40% A  
Damage level: 50% E



Damage location: L1  
Damage size: 100% A  
Damage level: 50% E

# Summary of FE Results

Sensitive/ insensitive modes for each damage location:

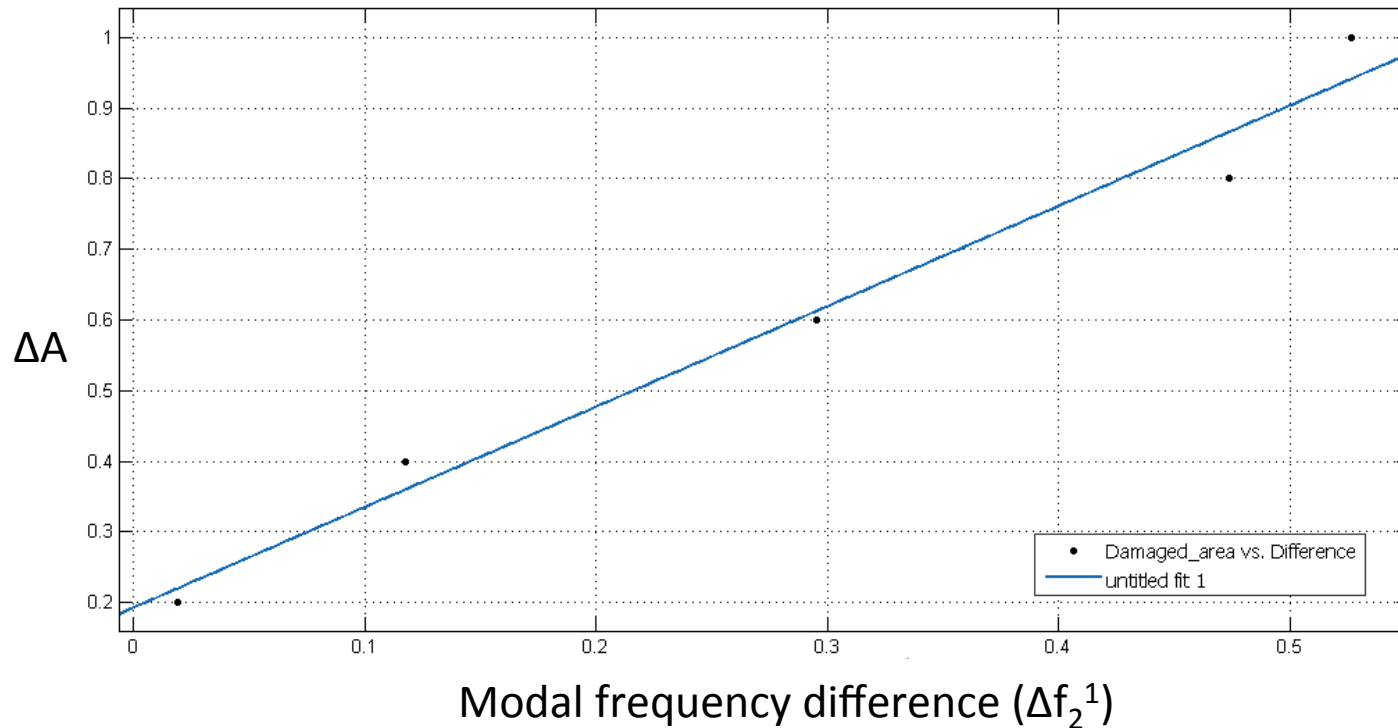
Table of sensitive/insensitive modes

Location	Sensitive modes	Insensitive modes
$L_1$	1, 7	6
$L_2$	1, 7	8, 10
$L_3$	9 or 10	7

→ The combination of sensitive modes and insensitive modes is **unique** for each damage location.

# Summary of FE Results

2-1. Linear relationships were developed between damage size and modal frequency difference.



# Quantification of Damages

Quantification of damage size  $\alpha$ :

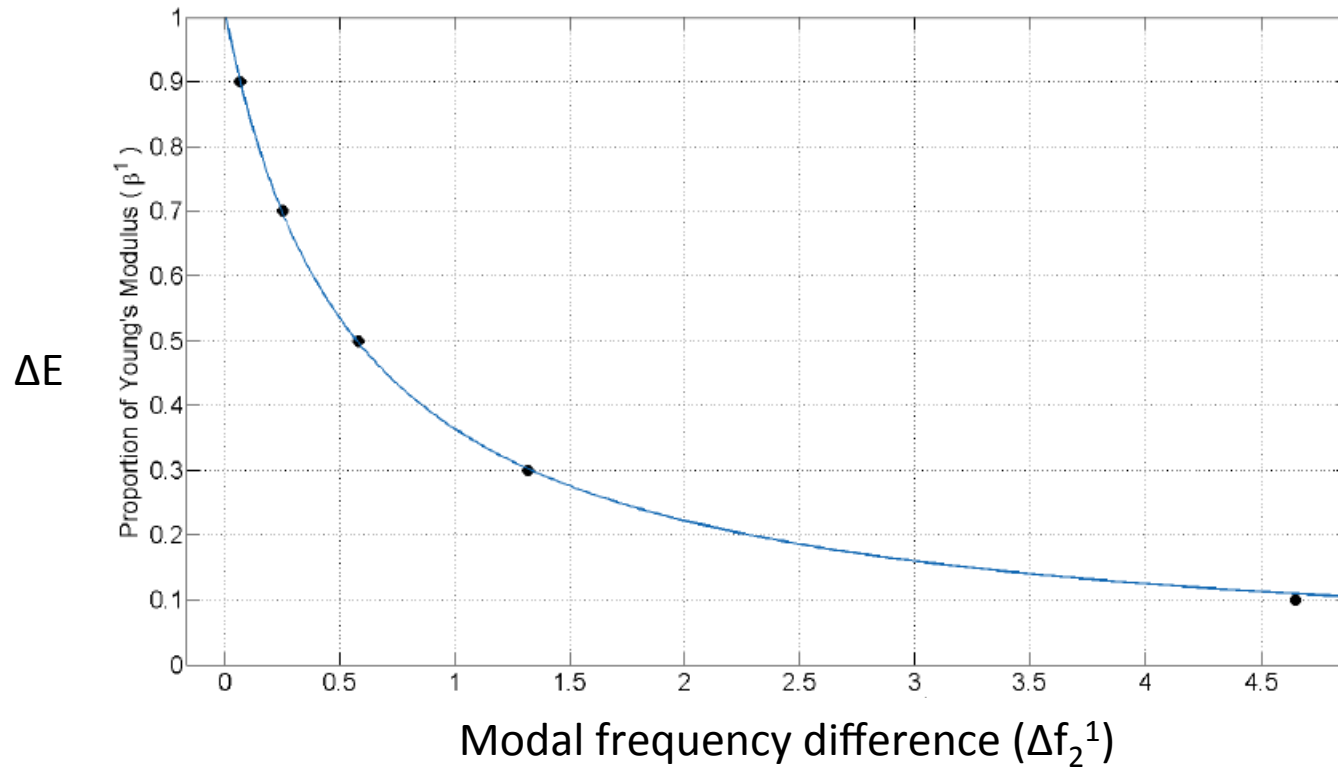
Linear relationships can be described by the following equation:

Damage size:  $\alpha^j = a\Delta f_i^j + b$

Location(j)	Best-fit mode(i)	$a$	$b$	$R^2$
1	10	0.0255	0.4614	0.9841
2	6	0.0526	0.1665	0.9966
3	4	0.6858	-0.1251	0.9750

# Quantification of Damages

2-2. Nonlinear relationships were developed between damage level (reduction in Young's modulus) and modal frequency difference.



# Quantification of Damages

Quantification of damage level  $\beta$ :

Relationship between damage level and modal frequency differences can be described by the following equation:

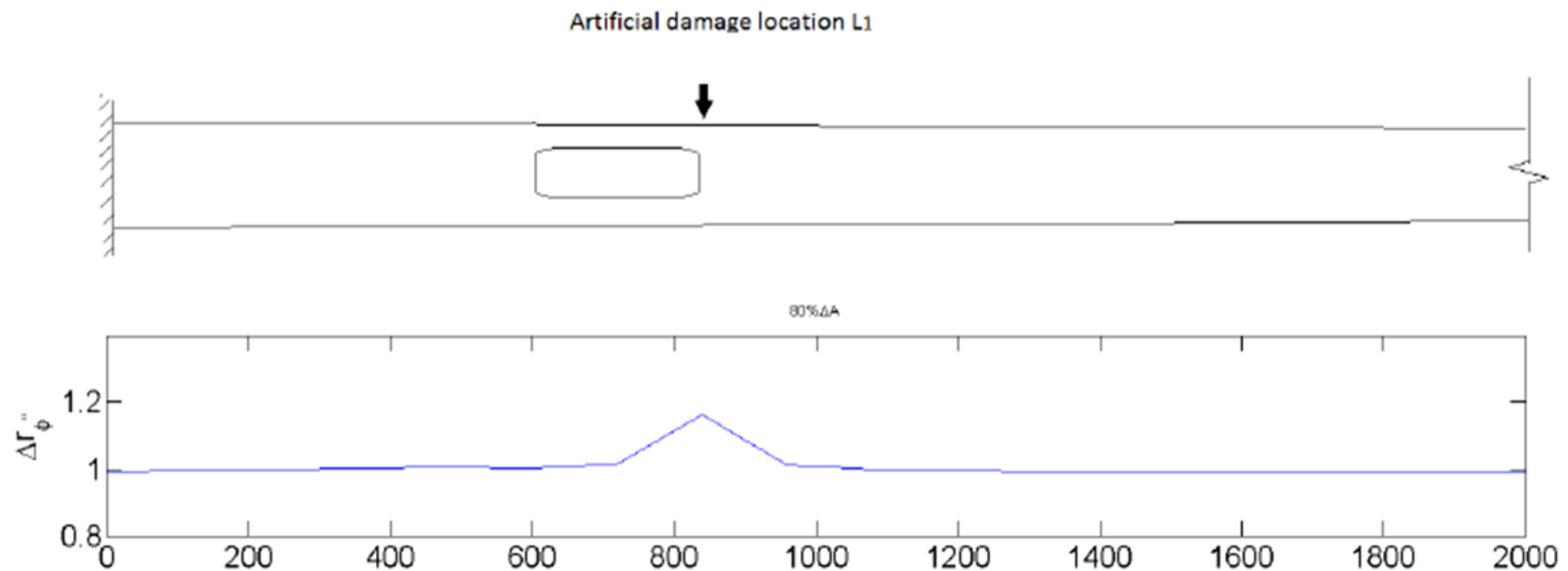
$$\text{Damage level: } \beta^j = c \ln(\Delta f_i^j) + d$$

Location(j)	Best-fit mode(i)	c	d	$R^2$
1	2	-0.195	0.3900	0.9911
2	2	-0.194	0.3879	0.9914
3	8	-0.199	0.3628	0.9914



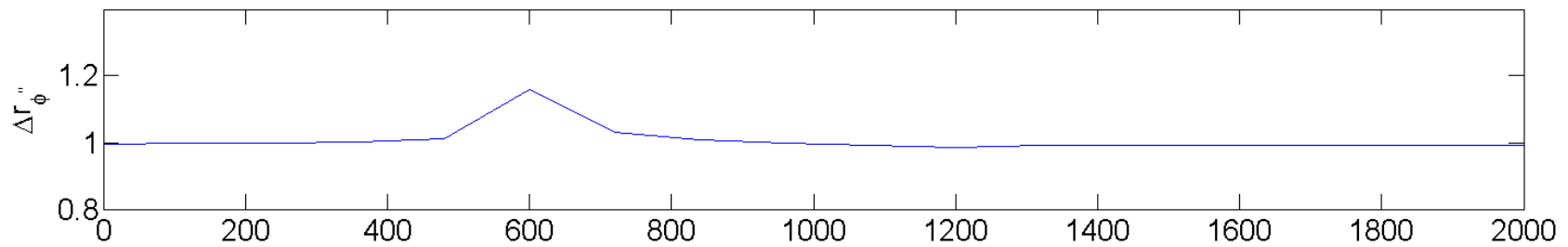
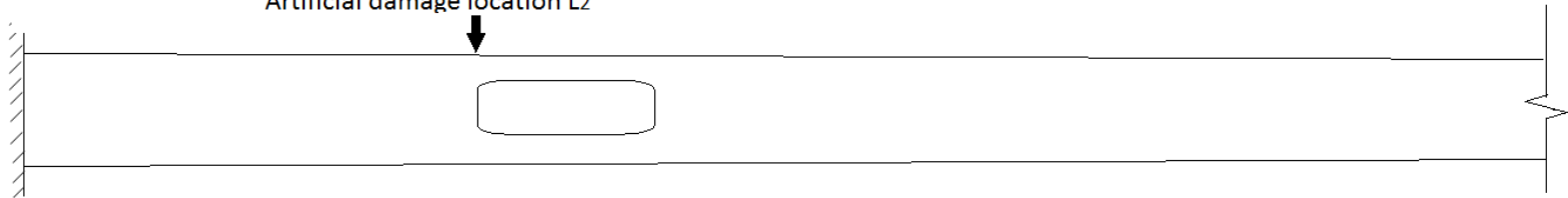
# Summary of FE results

3. Curvatures of the second mode shape changes the most ( $\Delta r_{\phi'' , \max}$ ) at damage location.

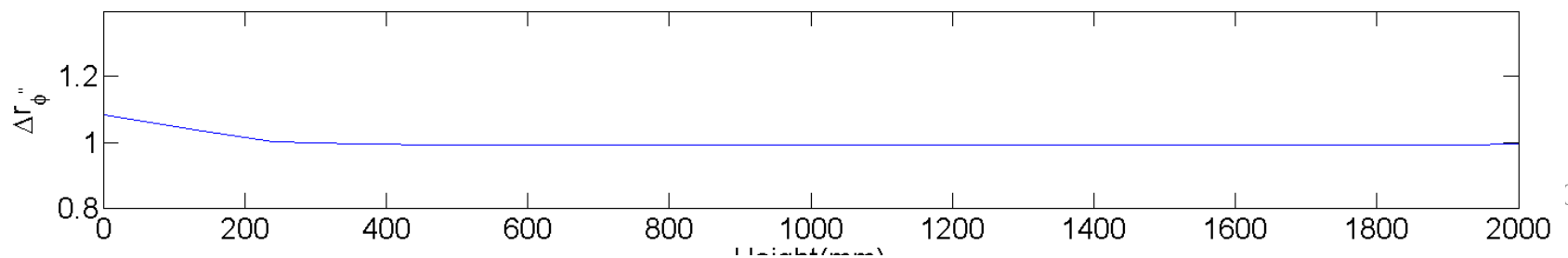
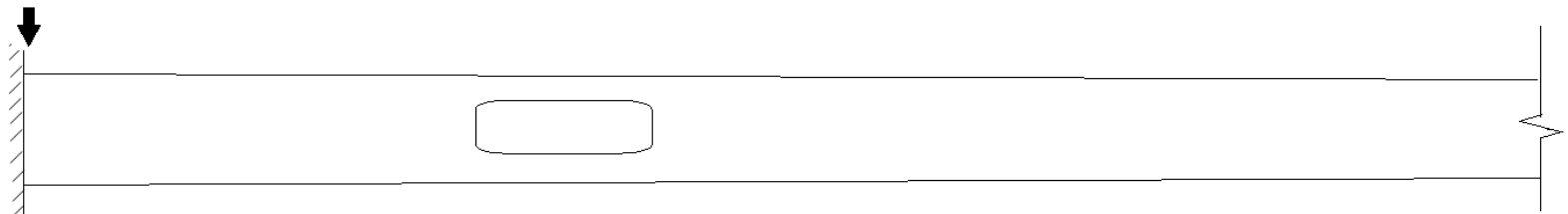


# Summary of FE results

Artificial damage location L<sub>2</sub>



Artificial damage location L<sub>3</sub>



# Special Case: Blind-test

- The intact light pole is unavailable.
- Modal frequencies of multiple light poles can always be obtained.
  - 1) Pick an arbitrary light pole as a baseline instead of the intact light pole.
  - 2) Use adjusted equation to compute modal frequency differences.

$$\Delta f_i^j = \left| \frac{(f_i^j|_{baseline} - f_i^j|_{damaged})}{f_i^j|_{baseline}} \right| * 100\%$$

- 3) Determine the sensitive/insensitive modes using moving thresholds  $t_s$  and  $t_i$ .
- 4) Check the following table and determine the damage location.

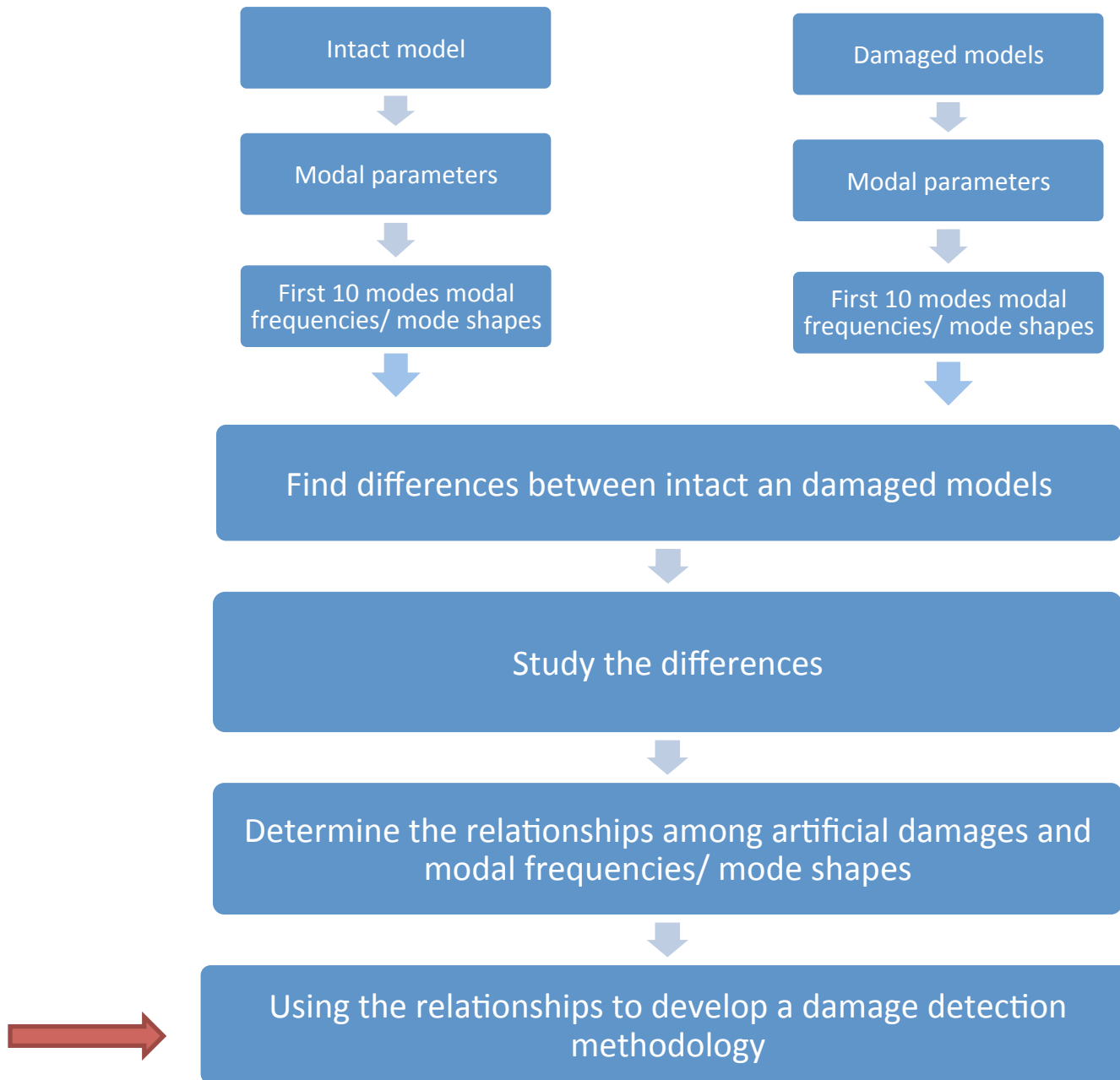
Location	Sensitive modes	Insensitive modes
L1	1,7	6
L2	1,7	8
L3	10	7

# Special Case: Blind-test

Constraints:

- Damages can only occur at  $L_1$ ,  $L_2$  or  $L_3$ .
- First ten modal frequencies of light pole are required.
- Damages can not be quantified.

# Roadmap



# Proposed Damage Detection Methodology

1. Extract first 10 **modal frequencies/ mode shapes** from an intact model & unknown models;
2. Compute the modal frequency differences and changes in mode shapes of the unknown light poles;
3. Compute thresholds  $t_s$  and  $t_i$ , and use them to identify sensitive/insensitive modes;
4. Locate the damage by checking the combination of sensitive and insensitive modes of unknown light poles in *Table of sensitive/insensitive modes*; or locate the damage by finding  $\Delta r_{\phi'', \max}$ ;
5. Use obtained empirical equations to quantify the damage.

# Conclusions

1. Locate damage using modal frequency -- Since the combination of sensitive modes and insensitive modes is unique for each damage location, one can locate the damage of light pole by checking the following table:

Table of sensitive/insensitive modes

Location	Sensitive modes	Insensitive modes
$L_1$	1, 7	6
$L_2$	1, 7	8, 10
$L_3$	9 or 10	7

# Conclusions

2. Quantify damage -- Substitute modal frequency difference into following equations:

Damage size:  $\alpha^j = a\Delta f_i^j + b$

Damage level:  $\beta^j = c \ln(\Delta f_i^j) + d$

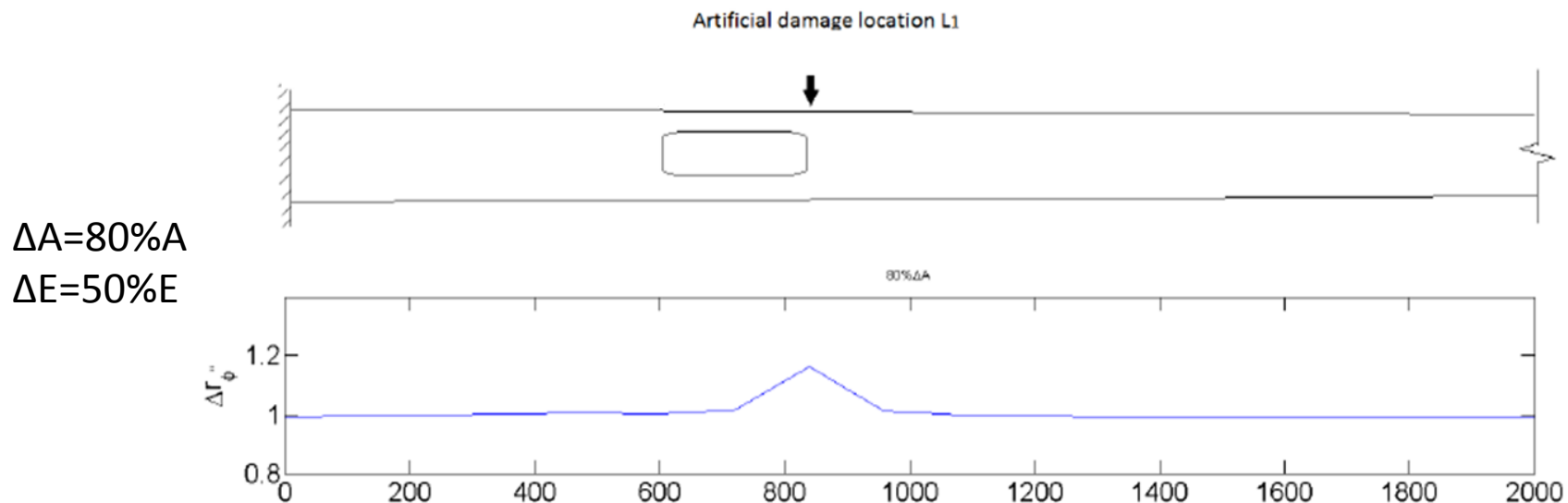
Location(j)	Best-fit mode(i)	<i>a</i>	<i>b</i>	<i>R</i> <sup>2</sup>
1	10	0.0255	0.4614	0.9841
2	6	0.0526	0.1665	0.9966
3	4	0.6858	-0.1251	0.9750

Location(j)	Best-fit mode(i)	<i>c</i>	<i>d</i>	<i>R</i> <sup>2</sup>
1	2	-0.195	0.3900	0.9911
2	2	-0.194	0.3879	0.9914
3	8	-0.199	0.3628	0.9914



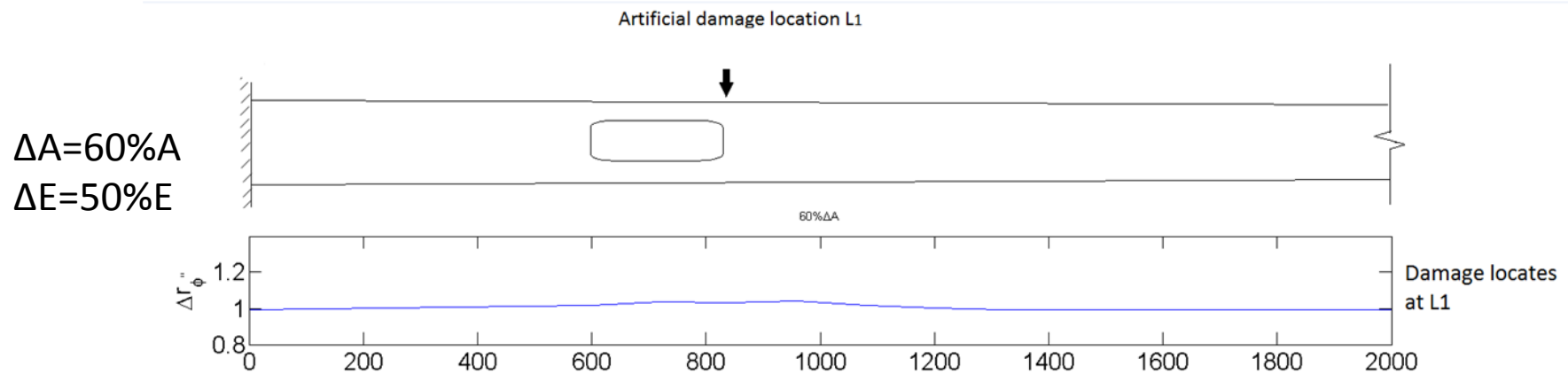
# Conclusions

3. Locate damage using mode shape curvature -- In the second mode, maximum curvature change ( $\Delta r_{\phi''}$ ,<sub>max</sub>) indicates damage location. Therefore, one can use changes in curvature of the second mode shape to locate damages. However, this method is **limited**.
- When damage size is greater than 80% of cross-sectional area, the maximum curvature changes accurately indicate damage locations.



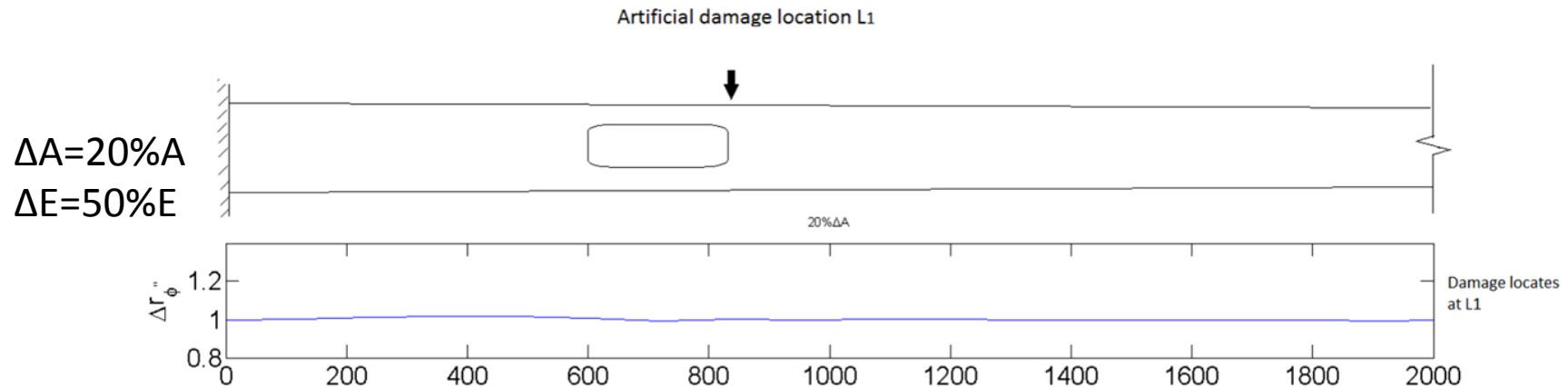
# Conclusions

- When damage size is between 40% to 60% of cross-sectional area, there will be shifts between the maximum curvature change location and damage location.



# Conclusions

- When damage size is smaller than 20% of cross-sectional area, the curvature change is not sensitive enough to locate the damage.



→ When  $\Delta A$  is smaller than 80%A, maximum curvature change ( $\Delta r_{\phi'', \max}$ ) of the second mode is not sensitive enough to locate damage.

# Contributions

- Sensitive modes and insensitive modes of light poles are defined, and their combinations are found to be unique for each damage location.
- Two empirical equations were proposed for damage quantification.
- A damage detection methodology is proposed to identify the damages in a light pole structure using its dynamic responses (modal frequencies and mode shapes) in free vibration.

# Future Work

- Conduct experiments to confirm the FE simulation results.
- Develop a method to quantify the damages (specifically, damage's size and level) using changes in mode shape curvature.
- Develop a damage detection methodology using fewer (e.g., 4) modal frequencies.
- Explore more damage locations (e.g., the conjunctive weld between pole and base plate).

# Acknowledgement

- I would like to express my sincere gratitude to my advisor Professor Tzuyang Yu for his invaluable help and support as well as his technical guidance, endless forbearance, and constant encouragement.
- I would like to thank my thesis committee: Prof. Avitabile and Prof. Inalpolat and Prof. Faraji for their insightful comments.
- My sincere thanks also go to my friends Jones Owusu Twumasi and Ross Gladstone, for their kind helps and useful suggestions.

# References

- [1] M. A. B. Abdo and M. Hori. A numerical study of structural damage detection using changes in the rotation of mode shapes. *Journal of Sound and Vibration*, 251 (2):227–239, 2002.
- [2] Y. Aoki and O. I. Byon. Damage detection of cfrp pipes and shells by using localized flexibility method. *Advanced Composite Materials*, 10 (2-3):189–198, 2001.
- [3] D. Armon, Y. Ben-Haim, and S. Braun. Crack detection in beams by rank- ordering of eigenfrequency shift. *Mechanical Systems and Signal Processing*, 8:81–91, 1994.
- [4] L. Caracoglia and N. P. Jones. Analysis of light pole failures in illinois - final report. Technical Report UILU-ENG-2004-2007, Department of Civil and Envi- ronmental Engineering University of Illinois at Urbana-Champaign, 2004.
- [5] E. P. Carden and P. Fanning. Vibration based condition monitoring: A review. *Structural Health Monitoring*, 3 (4):355–377, 2004.
- [6] Q. Chen and K. W. Y. W. Chan. Structural fault diagnosis and isolation using neural networks based on response-only data. *Computers Structures*, 81 (22- 23):2165–2172, 2003.
- [7] A. K. Chopra. *Dynamics of structures*. Third edition edition, 2007.
- [8] J. H. Chou and J. Ghaboussi. Genetic algorithm in structural damage detection. *Computers Structures*, 79 (14):1335–1353, 2001.
- [9] Dassault Systé mes, 10 rue Marcel Dassault, CS 40501, 78946 Ve´lizy- Villacoublay Cedex - France. Abaqus/CAE User’s Manual Version 6.11, <http://abaqus.ethz.ch:2080/v6.11/>.
- [10] H. V. der Auweraer. International research projects on structural damage detec- tion. *Damage Assessment of Structures Key Engineering Materials*, 204-2:97– 112, 2001.
- [11] M. R. K. et al. NCHRP report 412: Fatigue-resistant design of cantilevered sig- nal, sign and light supports. Technical Report HR 10-38, ATLSS Engineering Research Center, 1998.
- [12] M. L. Fugate, H. Sohn, and C. R. Farrar. Vibration-based damage detection us- ing statistical process control. *Mechanical Systems and Signal Processing*, 15 (4):707–721, 2001.
- [13] A. Furukawa, H. Otsuka, and J. Kiyono. Structural damage detection method using uncertain frequency response functions. *Computer- Aided Civil And Infras- tructure Engineering*, 21 (4):292–305, 2006.
- [14] M. J. Garlich and E. T. Thorkildsen. Guidelines for the installation, inspection, maintenance and repair of structural supports for highway signs, luminaires, and traffic signals. Technical Report FHWA NHI 05-036, Office of Bridge Technology Federal Highway Administration, 2005.

# References

- [15] P. Gudmundson. Eigenfrequency changes of structures due to cracks, notches or other geometrical changes. *Journal of Mechanics and Physics of Solids*, 30:339–53, 1982.
- [16] J. He and Z. F. Fu. *Modal Analysis*. Butterworth Heiemann, 2001.
- [17] A. Iwasaki, A. Todoroki, Y. Shimamura, and H. Kobayashi. Unsupervised structural damage diagnosis based on change of response surface using statistical tool (application to damage detection of composite structure). *SME International Journal Series A-Solid Mechanics and Material Engineering*, 47 (1):1–7, 2004.
- [18] C. Y. Kao and S. L. Hung. Detection of structural damage via free vibration responses generated by approximating artificial neural networks. *Computers Structures*, 81 (28-29):2631–2644, 2003.
- [19] L. M. Khoo, P. R. Mantena, and P. Jadhav. Structural damage assessment using vibration modal analysis. *Structural Health Monitoring*, 3 (2):177–194, 2004.
- [20] J. T. Kim, Y. S. Ryu, H. M. Cho, and N. Stubbs. Damage identification in beam-type structures: frequency-based method vs. mode-shapebased method. *Engineering Structures*, 25 (1):57–67, 2003.
- [21] J.-T. Kim and N. Stubbs. Crack detection in beam-type structures using frequency data. *Journal of Sound and Vibration*, 259 (1):145–160, 2003.
- [22] J. T. Kim, H. M. C. Y. S. Ryu, and N. Stubbs. Damage identification in beam-type structures: frequency-based method vs mode-shape-based method. *Engineering Structures*, 25:57–67, 2003.
- [23] S. S. Law, X. Y. Li, X. Q. Zhu, and S. L. Chan. Structural damage detection from wavelet packet sensitivity. *Engineering Structures*, 27 (9):1339–1348, 2005.
- [24] T. Lea, A. Abolmaalia, S. A. Motaharia, W. Yei hb, and R. Fernandezc. Finite element-based analyses of natural frequencies of long tapered hollow steel poles. *Journal of Constructional Steel Research*, 64:275–284, 2008.
- [25] Y. Lee and M. Chung. A study on crack detection using eigenfrequency test data. *Computers and Structures*, 64:327–342, 2000.
- [26] Y. S. Lee and M. J. Chung. A study on crack detection using eigenfrequency test data. *Computers Structures*, 77 (3):327–342, 2000.
- [27] T. Y. Li, T. Zhang, J. X. Liu, and W. H. Zhang. Vibrational wave analysis of infinite damaged beams using structure-borne power flow. *Applied Acoustics*, 65 (1):91–100, 2004.
- [28] J. Lopez-Diez, M. Torrealba, A. Guemes, and C. Cuerno. Application of statistical energy analysis for damage detection in spacecraft structures. *Damage Assessment of Structures Vi Key Engineering Materials*, 525-532:1-7, 2005.



# References

- [29] C. J. Lu and Y. T. Hsu. Vibration analysis of an inhomogeneous string for damage detection by wavelet transform. *International Journal of Mechanical Sciences*, 44 (4):745–754, 2002.
- [30] D. Mahapatra and S. Gopalakrishnan. Spectral finite element analysis of coupled wave propagation in composite beams with multiple delaminations and strip inclusions. *International Journal of Solids and Structures* 41, 5-6:1173–1208, 2004.
- [31] K. Moslem and R. Nafaspour. Structural damage detection by genetic algorithms. *AIAA Journal*, 40 (7):1395–1401, 2002.
- [32] G. M. Owolabi, A. S. J. Swamidas, and R. Seshadri. Crack detection in beams using changes in frequencies and amplitudes of frequency response functions. *Journal of Sound and Vibration*, 265:1–22, 2003.
- [33] N. G. Park and Y. S. Park. Identification of damage on a substructure with measured frequency response functions. *Journal of Mechanical Science and Technology*, 19 (10):1891–1901, 2005.
- [34] V. A. Pino. Fatigue life prediction of cantilevered light pole structures, 2010.
- [35] S. Rajasekaran and S. P. Varghese. Damage detection in beams and plates using wavelet transforms. *Computers and Concrete*, 2 (6): 481–498, 2005.
- [36] B. R. Reese. Non-destructive examination techniques of tubular steel pole sports lighting structures.
- [37] R.J.Connor, J.Ocel, and B.Brakke. Fatigue cracking and inspection of high-mast lighting towers. Technical Report IBC-05-31, Iowa and Pennsylvania Departments of Transportation, Pennsylvania Infrastructure Technology Alliance (PITA), 2005.
- [38] R. P. C. Sampaio, N. M. M. Maia, and J. M. M. Silva. The frequency domain assurance criterion as a tool for damage detection. *Proceedings Key Engineering Materials*, 245-2:69–76, 2003.
- [39] Z. Y. Shi, S. S. Law, and L. Zhang. Structural damage detection from modal strain energy change. *Journal of Engineering Mechanics ASCE*, 26:1216–1223, 2000.
- [40] Z. Y. Shi, S. S. Law, and L. M. Zhang. Structural damage detection from modal strain energy change. *Journal of Engineering Mechanics- ASCE*, 126 (12):1216– 1223, 2000.
- [41] J. Shortsleeve. I-team: Aging light poles a safety concern on Mass. roads. <http://boston.cbslocal.com/2012/10/31/>, 2012.
- [42] L. H. Yam, Y. J. Yan, and Z. Wei. Vibration-based non-destructive structural damage detection, advances in nondestructive evaluation. *Key Engineering Materials*, 270-273:1446–1453, 2004.
- [43] A. M. Yan and J. C. Golinval. Structural damage localization by combining flexibility and stiffness methods. *Engineering Structures*, 27 (12):1752–1761, 2005.

# References

- [44] Y. J. Yan, Z. Y. W. L. Cheng, and L. H. Yam. Development in vibration-based structural damage detection technique. *Mechanical Systems and Signal Processing*, 21:2198–2211, 2007.
- [45] Y. J. Yan and L. H. Yam. Online detection of crack damage in composite plates using embedded piezoelectric actuators/sensors and wavelet analysis. *Composite Structures*, 58 (1):29–38, 2002.
- [46] Y. J. Yan, L. H. Yam, L. Cheng, and L. Yu. Fem modeling method of damage structures for structural damage detection. *Composite Structures*, 72:193–199, 2006.
- [47] H. Z. Yang, H. J. Li, and S. Q. Wang. Damage localization of offshore platforms under ambient excitation. *China Ocean Engineering*, 17 (4):495–504, 2003.
- [48] M. K. Yoon, D. Heider, J. W. Gillespie, C. P. Ratcliffe, and R. M. Crane. Local damage detection using the two-dimensional gapped smoothing method. *Journal of Sound and Vibration*, 279:2198–2211, 2005.
- [49] K. Yuen and H. Lam. On the complexity of artificial neural networks for smart structures monitoring. *Engineering Structures*, 28:977–984, 2006.

# Appendix

Validation of sensitive modes:

Gudmunson [15] proposed the following equation which relates fractional changes in modal strain energy and modal frequency:

$$\frac{\delta W_i}{W_i} = \frac{\delta \omega_i^2}{\omega^2}$$

where  $W_i$  is the  $i$ th modal strain energy of the intact structure,  $\delta W_i$  is the loss in the  $i$ th modal strain energy after damage, and  $\delta \omega^2 / \omega^2$  is the fractional change in the  $i$ th eigenvalue (modal frequency difference) due to the damage.

$$\delta W_i \uparrow \longrightarrow \delta \omega_i^2 \uparrow$$

# Appendix

Kim *et. al.* [20] proposed following equation to compute  $\delta W_i$  of a simple supported beam structure:

$$\delta W_i = \left( \frac{\pi t (1 - \nu^2)}{2E} F^2 \sigma_k^2 a_k^2 \right)_i$$

in which, for the  $i$ th mode,  $a_k$  represents the damage size (depth) at location  $k$  and  $\sigma_k$  represents the maximum flexural stress at location  $k$  along the beam's longitudinal axis,  $t$  is the beam thickness,  $E$  is Young's modulus,  $\nu$  is Poisson's ratio and  $F$  is a geometrical factor depending on the dimensionless crack-length/beam-depth ratio  $a/H$ .

$\pi$ ,  $t$ ,  $\nu$ ,  $E$ ,  $F$ ,  $a_k$  are constant.



# Appendix

Therefore, the mode which have largest modal frequency difference  $\delta\omega_i$  has the maximum value of  $\Delta\sigma_k^2$  (difference between intact and damaged structures).

$$\delta\omega_{i, max}^2 \longrightarrow \Delta\sigma_{k, max}$$

# Appendix

The longitudinal stress of an arbitrary point  $m$  in this cross-section is:

$$\sigma_m = \frac{M(x)c_m}{I}$$

For an Euler-Bernoulli beam, its bending moment at location  $x$  is:

$$M(x) = -EI \frac{d^2\phi(x)}{dx^2} = -EI\phi''(x)$$

where  $E$  is Young's modulus,  $I$  is moment of inertia of the beam cross-section at location  $x$ ,  $\phi(x)$  is the displacement of the beam and  $\phi''(x)$  is the curvature of the mode shape.

$$\longrightarrow \sigma_m = -c_m E \phi''(x)$$

# Appendix

then,

$$\Delta\sigma_m = \frac{\sigma_m - \sigma_m^*}{\sigma_m} = \frac{-c_m E \phi''(x) - (-c_m E^* \phi''^*(x))}{-c_m E \phi''(x)} = 1 - j \frac{\phi''^*}{\phi''}$$

where  $E^*$  is Young's modulus of damaged materials, and  $j$  is the ratio between  $E$  and  $E^*$ .

Also,

$$\phi''(x)_n = \frac{\phi(x)_{n+1} - 2\phi(x)_n + \phi(x)_{n-1}}{d^2}$$

$$\frac{\phi''^*(x)_n}{\phi''(x)_n} = \frac{\phi^*(x)_{n+1} - 2\phi^*(x)_n + \phi^*(x)_{n-1}}{\phi(x)_{n+1} - 2\phi(x)_n + \phi(x)_{n-1}}$$

# Appendix

Let  $\phi^*(x)_n = \phi(x)_n + \delta_n$ , where  $\delta_n$  is the differential displacement between  $\phi^*(x)_n$  and  $\phi(x)_n$ ,

$$\begin{aligned}\frac{\phi''^*(x)_n}{\phi''(x)_n} &= \frac{(\phi(x)_{n+1} + \delta_{n+1}) - 2(\phi(x)_n + \delta_n) + (\phi(x)_{n-1} + \delta_{n-1})}{\phi(x)_{n+1} - 2\phi(x)_n + \phi(x)_{n-1}} \\ &= 1 + \frac{\delta_{n+1} - 2\delta_n + \delta_{n-1}}{\phi(x)_{n+1} - 2\phi(x)_n + \phi(x)_{n-1}}\end{aligned}$$

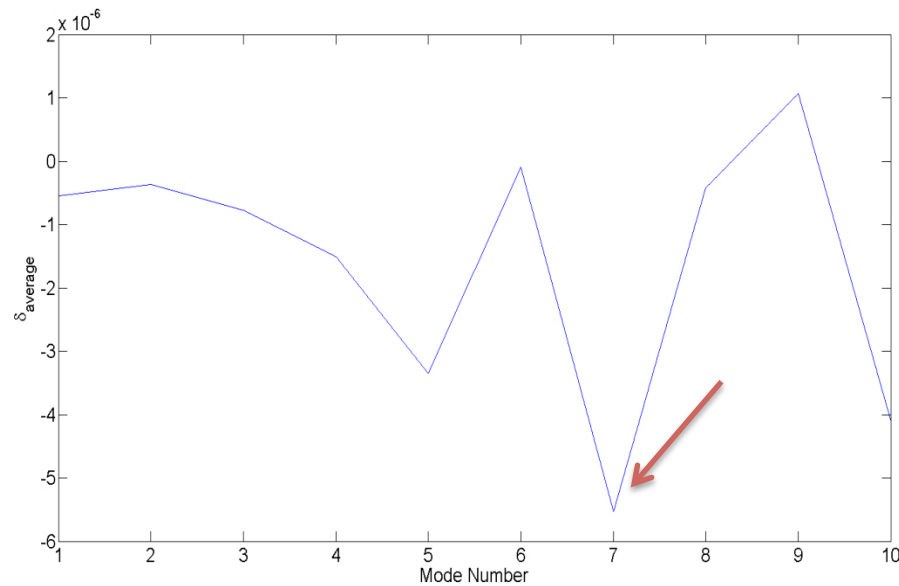
$$\delta_{n+1} - 2\delta_n + \delta_{n-1} \Big|_{\min} \quad \longrightarrow \quad \frac{\phi''^*(x)_n}{\phi''(x)_n} \Big|_{\min} \quad \longrightarrow \quad \Delta\sigma_{k, \max} \quad \longrightarrow \quad \delta\omega_i^2_{\max}$$



# Appendix

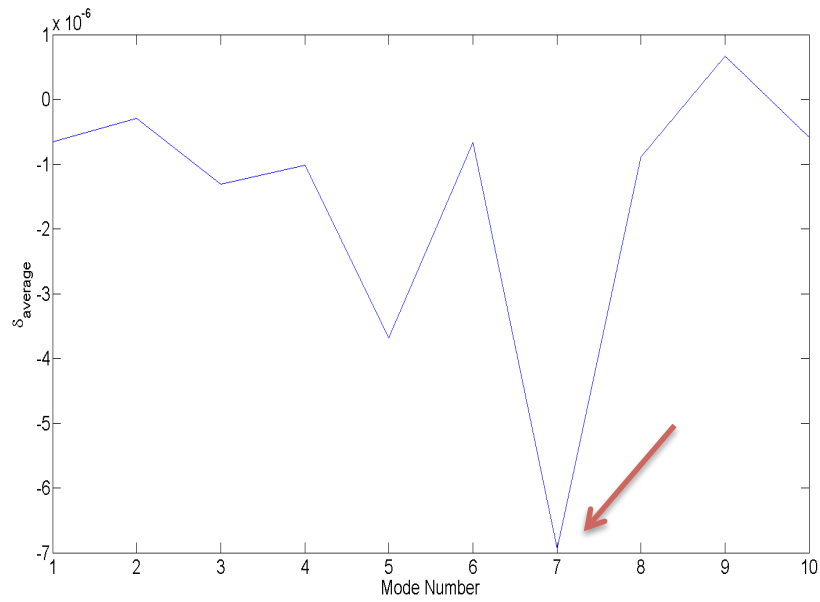
Example: Damage scenario A-5 ( $\Delta A=100\%$ ,  $\Delta E=50\%$ ).

The modes with the minimum value of  $\delta_{n+1} - 2\delta_n + \delta_{n-1}$  for each damage location are:  $L_1-7^{\text{th}}$  Mode;  $L_2-7^{\text{th}}$  Mode; and  $L_3-10^{\text{th}}$  mode.

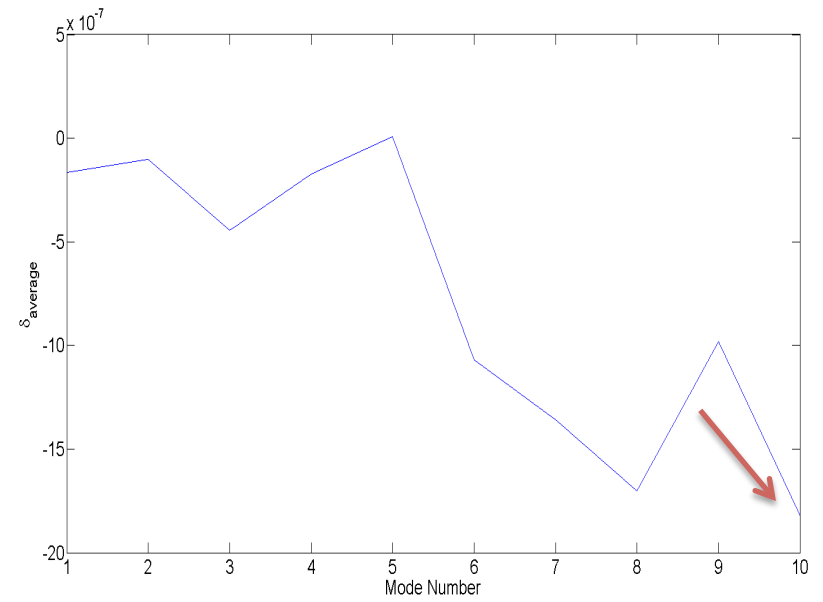


$L_1-7^{\text{th}}$  Mode

# Appendix



$L_2-7^{\text{th}}$  Mode



$L_3-10^{\text{th}}$  mode

# Appendix

Compare with the most sensitive modes identified from FE models, the theoretical derivation results show a good agreement with FE results.

	Most sensitive mode	Minimum $\delta_{\text{average}}$
L1	7th mode	7th mode
L2	7th mode	7th mode
L3	10th mode	10th mode